Aerial Radiological Survey of Defense-Related Uranium Mines in the Shirley Basin, Crooks Gap, and Gas Hills Regions in Wyoming

Final Report

U.S. Department of Energy
National Nuclear Security Administration
Remote Sensing Laboratory
Aerial Measuring System
December 30, 2021

This work was done by Mission Support and Test Services, LLC, under Contract No. De-NA0003624 with the U.S. Department of Energy, and the Office of Legacy Management
DOE/NV/03624–1395

National Nuclear Security Administration

Contents

List of Figures

List of Tables

List of Equations

Introduction

Defense-Related Uranium Mines program

The United States (U.S.) Department of Energy (DOE) Defense-Related Uranium Mines (DRUM) program is a partnership between DOE, federal land management agencies, state abandoned mine lands (AML) programs, and tribal governments to verify and validate the condition of a unique set of abandoned uranium (U) mines. These mines provided U ore to the U.S. Atomic Energy Commission (AEC) for defense-related activities. Many of these mines are located on public land. The primary objective of the DRUM program is to inventory and sample an estimated 4,000 abandoned uranium mines and screen them for potential health hazards caused by residual heavy metals or radiological elements.

Initiated in 2017, DRUM Campaign 1 has focused on approximately 2,500 legacy mines located on public land administered by federal and state agencies. DRUM Campaign 2, scheduled to commence fieldwork in fiscal year (FY) 2023, will assess DRUM sites on tribal land. Finally, DRUM Campaign 3 will address DRUM sites on private property and is scheduled to begin fieldwork in FY 2024.

The DRUM program is managed by the DOE Office of Legacy Management (LM), and is implemented by conducting verification and validation (V&V) activities, including:

- Exchanging information with other federal agencies and state governments to improve the quality of mine-specific data.
- Performing field inventories to document the condition of the mines.
- Conducting gamma surveys, soil sampling, and water sampling (as applicable).
- Producing mine-specific reports that offer inventory results, as well as evaluations of physical hazards and potential chemical and radiological risks.

Ultimately, these V&V activities will result in preliminary risk screening to assess whether the mines pose potential risks to human health and the environment. This information will be shared with the Bureau of Land Management (BLM), U.S. Forest Service, and state and tribal governments and will inform decisions addressing any risks found at the mines.

A typical DRUM site ranges from 1-6 acres. DRUM inventory and sampling procedures were designed to accommodate these relatively small sites. However, large DRUM sites in Wyoming are often measured in square miles, which increases the cost of current sampling procedures significantly. Therefore, LM requested assistance from the National Nuclear Security Administration (NNSA) Aerial Measuring System (AMS) to provide aerial gamma

survey expertise to map the terrestrial gamma signature and other related radiological attributes of these large areas. This information will be used to prioritize LM's follow-up ground-based sampling program. LM currently manages nine sites where remediation was conducted in accordance with Comprehensive Environmental Response, Compensation, and Liability Act (CERCLA) and/or Resource Conservation and Recovery Act (RCRA) regulations. These sites were radiologically and/or chemically contaminated by federal milling, processing, research, and/or weapons manufacturing operations.

Scope of the aerial measurement campaign

The primary objective for AMS was to provide an aerial gamma ray survey via helicopter that accurately maps the spatial distribution of terrestrial radiation in units of μR/hr (exposure rate), total counts, and excess bismuth (^{214}Bi) over the survey areas. The survey flight parameters were set such that a resolution one-acre per field of view was achieved, with a minimum reportable activity of less than 5 μR/hr. These data will enable the DRUM program to identify areas that could be targeted for follow-up ground-based sampling. Specific exposure-based benchmarks used by the DRUM program were used to assist the survey design, as well as the survey mapping and reporting requirements. These benchmarks are based upon the recreational camping scenario and are: 32 μR/hr, 64 μR/hr and 256 μR/hr.

AMS collected spectral gamma ray data in 1024 channels over an energy range of 20 to 3070 keV. Total terrestrial exposure rate is calculated from empirical conversion factors on spectra over the range of 24 to 3066 keV. Concentration extractions were generated using both the standard International Atomic Energy Agency (IAEA) spectral extraction method [9] and the Gaussian Extraction method for internal verification of the results. The isotopic extractions for potassium (K), equivalent uranium (eU), and equivalent thorium (eTh) are generated in units of weight percent (Wt%) for K, and parts per million (ppm) for eU, and eTh. The total terrestrial exposure rate at 1 m above the ground was calculated by two methods: the standard AMS two-factor empirical exposure parameters, and by summing the exposure contribution calculated from the isotopic contributions of K, eU, and eTh.

AMS reported all flight data for the General Services Administration's Federal Aviation Interactive System database. The date and the number of flight hours for each survey are reported in Table 2. Flight hours for each survey are expressed in hours and tenths of an hour from the time which the aircraft moved under its own power for flight, and ends when the aircraft came to rest after landing. AMS provided LM draft maps of the proposed flight lines in March 2021. The initial survey areas were defined by LM in Figure 1 to include four survey

regions: Shirley Basin, Crooks Gap, Gas Hills North, and Gas Hills South. The two Gas Hills surveys are in close proximity, therefore, AMS merged the Gas Hills surveys resulting in fewer aircraft turns and lower overall required flight time in the Gas Hills region, while also providing additional data. The merged Gas Hills survey boundary can be seen in Figure 2. The individual planning maps for Shirley Basin, Crooks Gap, and Gas Hills can be found in Figures 3, 4, and 5 respectively.

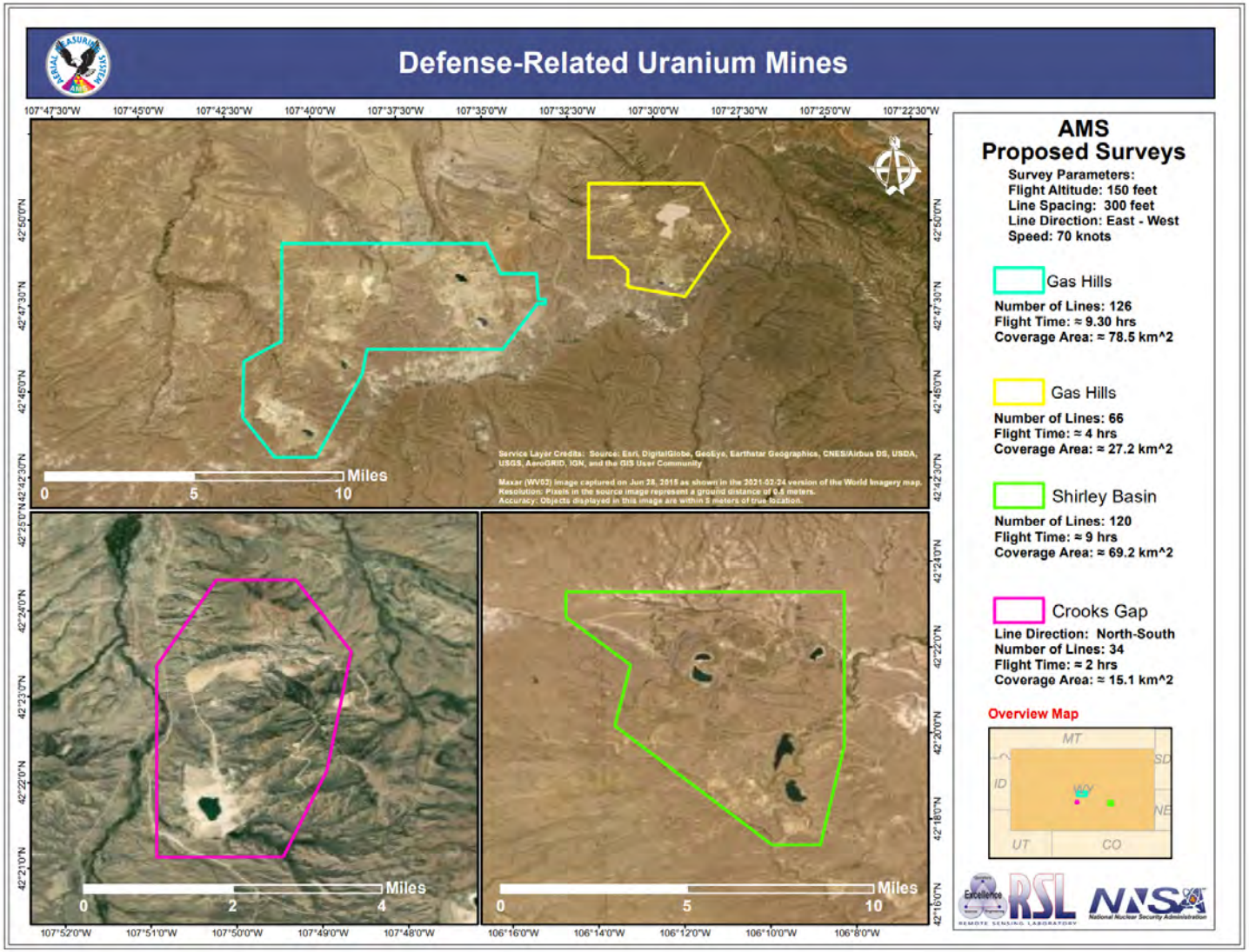

Figure 1: Initial LM survey plan with four survey regions: Shirley Basin, Gas Hills North, Gas Hills South, and Crooks Gap.

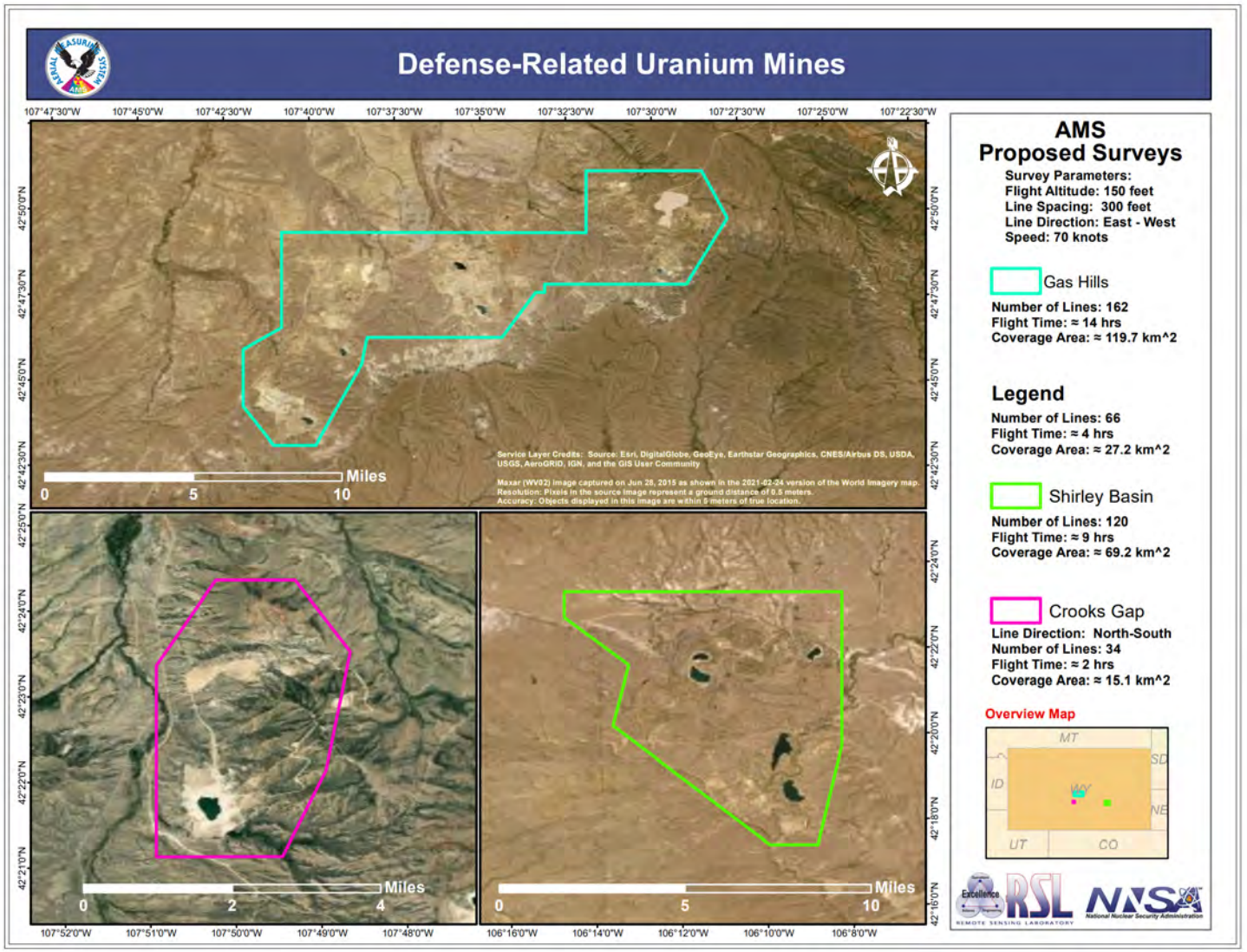

Figure 2: AMS survey plan combining Gas Hills to a single survey. Shirley Basin and the Crooks Gap survey remained unchanged.

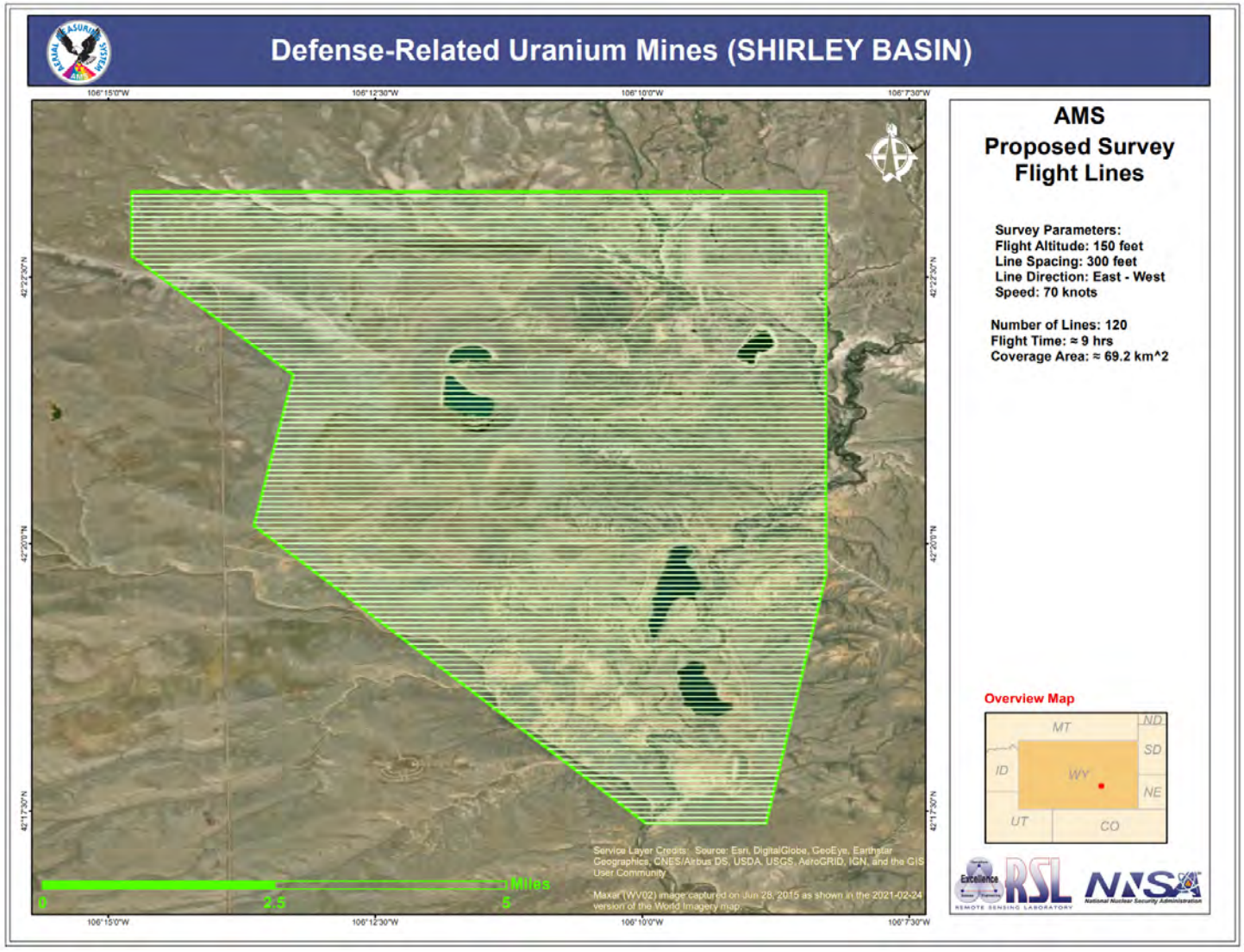

Figure 3: AMS survey plan for Shirly Basin survey.

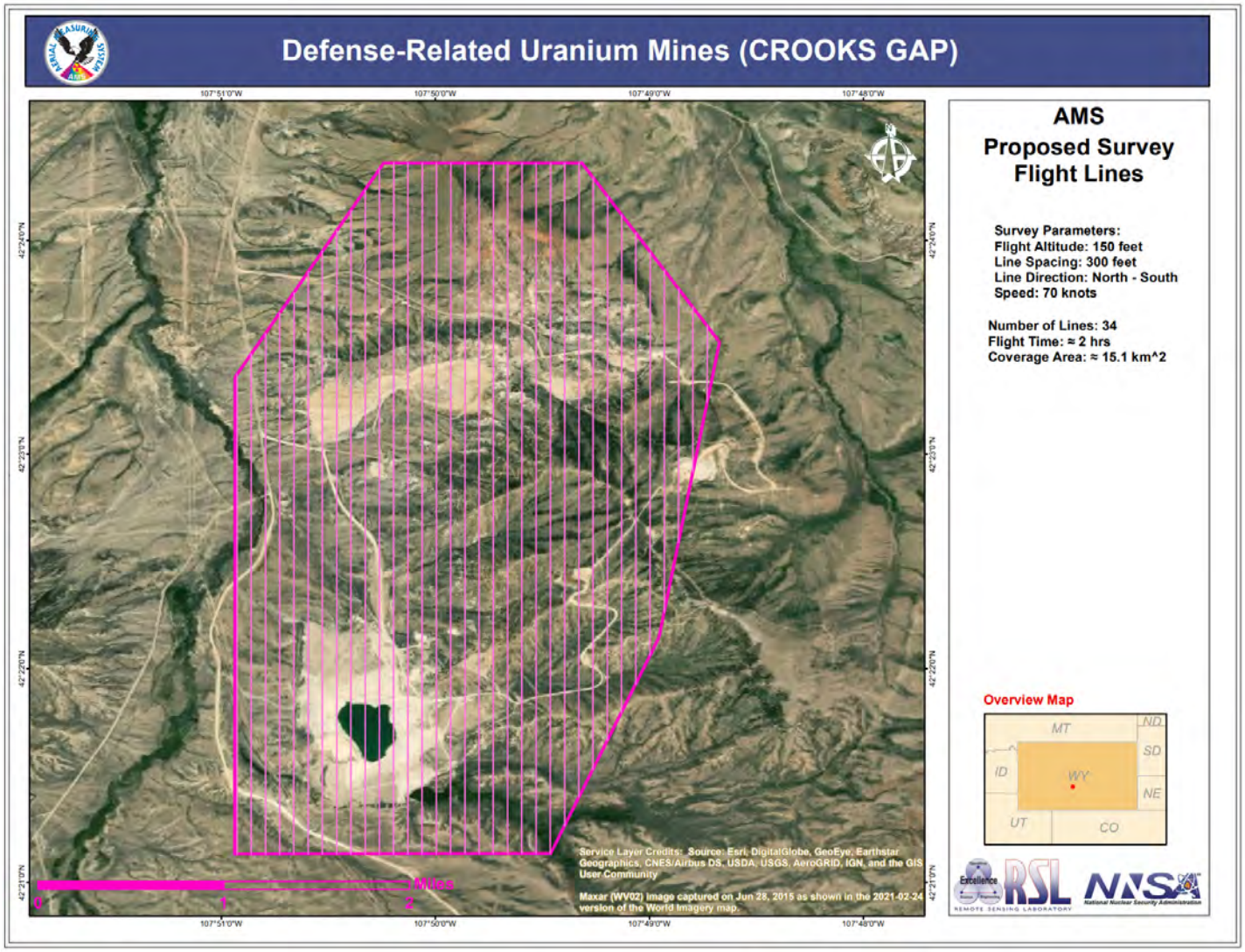

Figure 4: AMS survey plan for Crooks Gap survey.

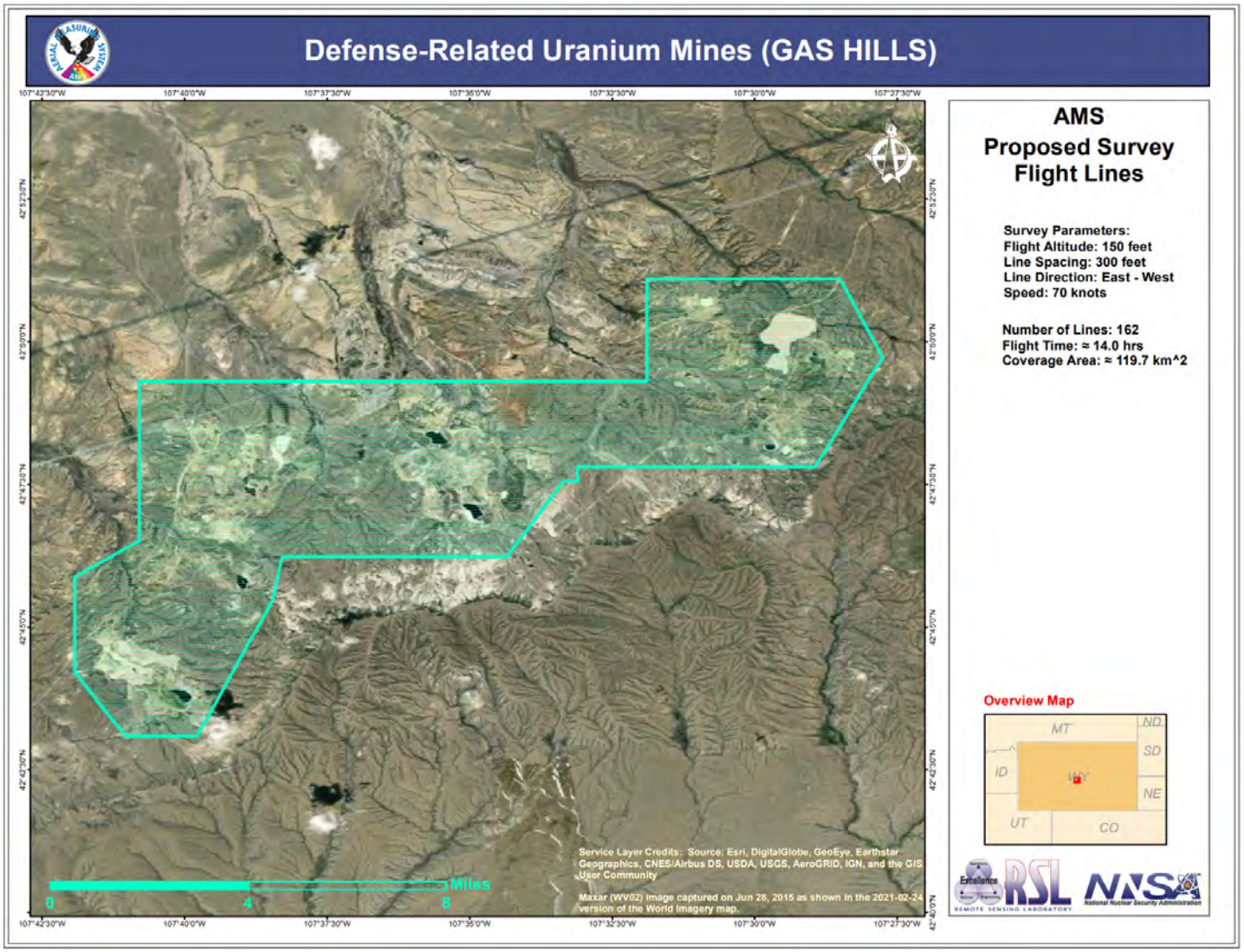

Figure 5: AMS survey plan for the combined Gas Hills survey.

Figures 3, 4, and 5 detail the mine survey areas and proposed flight lines. Table 1 summarizes the survey areas, line length in kilometers and estimated flight times for each location. Actual flight times for each flight of the survey are presented in Table 2. Total flight time is split nearly evenly between the time on survey and the transit time, which included background correction data collection.

Table 1: Estimated survey and transit flight times

DRUM Locality	**Coverage Area (acres)**	**Estimated Flight Line [km]**	**Estimated Flight Time [hr]**
Shirley Basin	17,100	1,185	9
Crooks Gap	3,731	263	2
Gas Hills East	6,721	526	4
Gas Hills West	19,398	1,224	9
Total*	46,950	3,198	60

*Transit from Nellis AFB and Casper WY included.

Table 2: Project survey flight times and on survey hours

Location	Date	Survey Flight #	Flight Time [h]	On Survey [h]
Shirley Basin	8/6	1	2.3	1.1
	8/6	2	1.6	0.8
	8/7	3	2.6	1.3
	8/7	4	2.7	1.8
	8/7	5	2.2	1.0
	8/8	6	2.6	1.3
	8/8	7	2.4	1.4
			16.3	**8.6**
Crooks Gap	8/8	8	1.7	0.2
	8/10	9	2.3	1.0
	8/10	10	1.9	1.0
	8/10*	11	0.8	
			6.7	**2.2**
Gas Hills	8/10	12	2.1	1.1
	8/11	13	2.6	1.4
	8/11	14	2.6	1.5
	8/12	15	2.0	0.8
	8/12	16	2.3	1.1
	8/12	17	1.6	0.6
	8/14	18	1.3	0.5
	8/16	19	2.4	1.1
	8/16	20	2.6	1.6
	8/16	21	1.8	0.7
	8/17	22	2.4	1.1
	8/17	23	2.3	0.9
			26.0	**12.4**
Nellis to Casper	8/5		**5.5**	
	8/20		**5.5**	
Totals			**59.8**	**23.2**

*Transit from Rawlins Airport to Casper Airport includes a water line flight.

AMS objectives defined in the statement of work:

- Generate maps for the three survey locations to include terrestrial gamma measurements defined in exposure rate (μR/hr) plotted using the DRUM benchmarks of $<$ 32, 32 to 64, 64 to 256, and greater than 256, and the total site estimated acreage exceeding these benchmarks.
- Identify possible spatial trends on-site and leading off-site in reference to the designated exposure rate benchmarks and excess ^{214}Bi that could be used in determining additional ground-based sampling.
- Identify locations of excess U through eU concentration estimates determined from the ^{214}Bi gamma ray lines, anomalies, and estimates of total site acreage of these anomalies.
- Excess ^{214}Bi is defined in terms of average eU above some nominal background. AMS will report estimated average concentrations and terrestrial exposure rate due to U and its daughters. A baseline of 3.5 μR/hr and 6 ppm will be used for the exposure rate and eU concentration respectively.

Summary of results

The AMS surveys at Shirley Basin, Crooks Gap, and the Gas Hills did not result in the discovery of any areas exceeding 256 μR/hr total terrestrial exposure rate and therefore no areas were identified where the contribution to exposure rate from U and its daughters exceeded that value. The total terrestrial exposure rate was calculated using a single background corrected energy window using the AMS standard methodology. The isotopic concentration estimates and uranium exposure contribution were generated using a Gaussian Extraction method and parameters derived from calibration at the DOE LM Large Area Calibration Pads (LACP) in Grand Junction, CO. All three surveys required multiple flights and at least two days to complete. In order to show continuity between the analysis for each flight, the last line of the previous flight was used as the first line of the next survey. The maximum difference in estimated total exposure rate on repeated survey lines was $<$2 μR/hr for the total terrestrial exposure estimate. The maximum concentration difference for the eU concentrations was found to be $<$3 eU(ppm) for repeated flight lines on the same survey. The estimated exposure rate and concentration differences are less than the expected uncertainty in these repeated line measurements. A full summary of the land area per exposure rate contour is presented in Table 3. The average equivalent uranium ranges correlated to the exposure ranges is also presented. The final maps for each survey area are presented in the Map Products and Results section.

Table 3: Acres per exposure zone and approximate eU concentrations

Exposure Benchmark [μR/hr]	Acres Per Contour			eU [ppm]
	Shirley Basin	Crooks Gap	Gas Hills	
0 to 32	17050	3400	27670	0 - 40
32 to 64	50	300	1860	75 -150
64 to 256	0	30	50	150 - 600
$>$ 256	0	0	0	$>$600
Total	17100	3730	29580	

Aerial Radiation Detection System

Aerial Measurement System Description

The Aerial Measuring System (AMS) acquisition platform consists of a DOE owned and mission dedicated Bell 412 helicopter and Radiation Solutions Incorporated (RSI) developed radiation detector system [13]. RSI systems are used worldwide for national security and geophysical research purposes. The AMS detection platform employs a total of 12 thallium doped sodium iodide (NaI(Tl)) crystals with dimensions of $2'' \times 4'' \times 16''$. These detectors are packaged in four RSX-3 units containing three crystals each and controlled by an RS-701. An RS-501 aggregator box combines the inputs of each RSX-3/RS-701 unit and also provides power distribution and differential GPS which is used to coordinate timing for data acquisition. The four RSX-3 boxes are fitted into the externally-mounted aluminum pods (two RSX-3 systems per pod) on both the left and right sides of the Bell 412 helicopter as seen in Figure 6. The AMS platform uses a radar altimeter for vertical positioning, referred to as above ground level (AGL) altitude or average height above the ground, and Differential Global Positioning Systems (DGPS) for location.

Each $2'' \times 4'' \times 16''$ NaI(Tl) crystal is coupled to a photomultiplier tube that produces analog voltage signals for digital analysis by the Advanced Digital Spectrometer (ADS) module. An open RSX-3 can be seen in Figure 7 (b). Each individual NaI(Tl) detector has its own high-speed (60 MHz) analog-to-digital converter and a Digital Signal Processor (DSP)/Field-Programmable Gate Array (FPGA) assembly. This module converts the analog signal from the detector to a digital spectrum with a 10^6 channel resolution. Using a unique detector energy calibration curve stored in the ADS module, the spectrum is linearized and compressed to the system's native 1024 channels. The high-speed adaptive DSP allows each pulse to be

(a) Bell 412 Helicopter

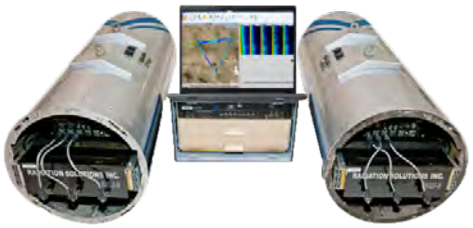

(b) RSI radiation sensors, RSI-501 console, and acquisition laptop

Figure 6: The AMS standard acquisition system for environmental surveys is based on the Bell 412 platform (a) and a 12 2″x4″x16″ NaI(Tl) system (b)

corrected, without significant distortion at very high data-throughput rates, up to 2,500,000 counts per second (cps) per crystal detector. The resulting spectra have very low dead time, improved pulse pileup rejection, and individual crystal linearization. These spectra are fed by 1 Mbps RS-485 data connections to the RS-701 console. The detector processing unit continuously monitors the state of health of the individual crystals and the system. Each crystal is individually gain-stabilized using a multi-peak approach, reducing the need for any pre-stabilization with external sources.

Integrated console (RS-701)

Each of the four RSX-3 units is controlled by the RS-701 console mounted on top of the RSX-3 box (Figure 7 (a)). The console uses RSI proprietary analysis techniques to automatically adjust the gain of the detectors to compensate for changing temperature and aging drift effects. The system uses spectra of naturally occurring radiological material (NORM) consisting of isotopes of potassium (K), uranium (U), and thorium (Th) present in all ground material to stabilize the system at startup and maintain this gain automatically during system use with no user input required. Each RS-701 console has a built-in GPS receiver. However, as the AMS RSI system integrates multiple RS-701 consoles into the RS-501 aggregator, the built-in GPSs are used only as synchronizing timers and not for positioning.

(a) RSI-701 Console on the RSX-3

(b) Exposed Indiviudal crystals and photomultiplier tubes

Figure 7: The RSI RSI-701 console (a) and open RSI RSX-3 with individual crystals and photomultiplier tubes exposed after the carbon fiber cover is removed (b)

Aggregator (RS-501)

Four RS-701 consoles are integrated into a single RS-501 aggregator, shown in Figure 6. The RS-501 aggregator combines the inputs of each RSX-3/RS-701 unit together, and provides a power distribution unit and differential GPS. The RS-501 unit retains 96 15-minute files representing the last 24 hours of data acquisition recorded to a solid-state disk in a 24-hour circular buffer. The RS-501 is then finally interfaced with the laptop PC running the Advanced Visualization and Integration of Data (AVID) software used for system monitoring and real-time data display in flight. The RS-501 console is shown in Figure 6 (b) along with a laptop running AVID.

AVID software

The AVID framework and associated modules were developed, as a joint effort between the Remote Sensing Laboratory (RSL) and Pacific Northwest National Laboratory (PNNL), for real-time acquisition, visualization, and analysis of radiation data from aerial and mobile detection systems. The AVID software is designed to support both data acquisition and analysis functionality for radiation detection systems. It is extensible and flexible in order to provide for the integration of various modules. Currently, the AVID software (version 2021) and associated modules are focused toward radiation detection instrumentation in support of NNSA mission objectives. The software provides an integration platform that allows developers within the NNSA Emergency Response community to develop modules for

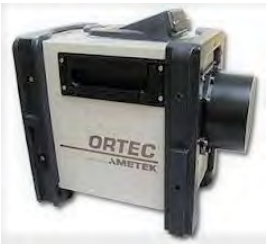

(a) Detective-200

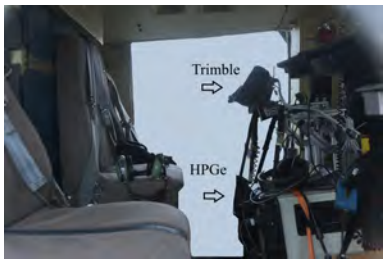

(b) Bell 412 helicopter interior

Figure 8: The Detective-200 HPGe (a) and Bell 412 interior showing the Trimble and HPGe systems (b)

incorporation into the AVID software package, thus facilitating the re-use of existing software resources while migrating toward an integrated system approach. AVID saves all the acquired data in the Microsoft SQL Server database, and supports several methods for exporting data to a variety of file formats (N42, CSV, KML, ESRI shape files) for use in other applications. As AVID is a pure acquisition software ("system agnostic"), the RSI RadAssist software is used to configure the RS-501 aggregator console via Ethernet link. AVID is used to link RSI data to other detector systems such as an Ortec high purity germanium (HPGe) spectrometer.

High purity germanium detector

An additional mechanically cooled HPGe called the Detective-200 is used in parallel to the RSI. The Detective-200 is a high resolution P-type high purity germanium crystal detector with a built-in removable 120 degree collimator which reduces airborne background interference and limits the field of view. This system utilizes a Marvel 806 MHz XScale processor and digital MCA with a proprietary digital spectrum gain stabilizer with 8K channels. The Detective-200 has a built in exposure estimator with two detectors used to determine the gamma dose rate over a wide range from < 5 μrem/h to >1 rem/h. For low dose rates, below $\sim$2 mrem/h, the dose rate is determined from the Ge detector spectrum. For higher dose rates an internal compensated GM tube is used to estimate dose. The manufacturer dose rate uncertainty is –50 % to +100 %. Data is collected from the Detective-200 in sync with the RSI detection system timing and GPS data through the AVID acquisition software. The high resolution and low efficiency of this detector can help to identify radionuclides in high count rate regimes. Detective-200 data was collected for the entire Shirley Basin and Crooks Gap surveys; because of equipment issues a small portion of Gas Hills was not covered by this instrument.

Pressurized ion chamber

The standard AMS methodology for measuring exposure rate in-situ is to use a pressurized ion chamber (PIC). AMS uses the RS-S131-200 which is a high-pressure argon gas system used to detect exposure rate due to gamma rays [5]. It is generally assumed that directional effects of the environmental radiation will not on average dominate the measurement and that measurements generated in the ion chamber will instead be dominated by the average incident photon flux and incident energy. This assumption is reasonable due to the spherical shape of the detector. However, the packaging and internal sensors will have some minimal impact on the angular response of the system. The photon energy response for the RS-S131-200 is relatively flat, but it does vary from 60 keV to 10,000 keV where the energy response drops off sharply below 60 keV. The calibration of this detector is referenced to ^{226}Ra making it ideal for in-situ measurements at a uranium mine facility. AMS operation of the PIC involves the use of a custom built stand, where the PIC is positioned 1-m above the ground for a minimum of 5 minutes to complete a measurement. In-situ measurements were completed for this project by AMS for validation of aerial measurements at Shirley Basin.

Methodology

Aerial gamma surveying

Three aerial surveys were performed over Defense-Related Uranium Mines (DRUM) sites in Wyoming. The spatial resolution of a survey is a function of three flight parameters; the AGL, the line spacing of the grid, and the speed. To achieve the desired resolution of 1 acre the flight parameters of the surveys were chosen to be an altitude of 150 ft AGL, line spacing of 300 ft, and speed of 70 knots. Gamma ray data were collected with spectral information up to 3 MeV and channeled into 1024 channels. The raw gamma spectra were processed to derive estimates of total exposure rate and concentrations of K, equivalent uranium (eU), and equivalent thorium (eTh).

Spectral extractions

The Lake Mohave calibration range in Nevada allows AMS to calibrate the detection system for count to exposure rate and height attenuation via empirical measurement. To obtain the total exposure rate from the spectral measurements, a count to exposure rate coefficient, determined at Lake Mohave, was applied to the sum of the spectrum counts from 24 to 3066

keV. The data were then corrected to 1m AGL by applying an exponential fit using the height attenuation coefficient also obtained from the Lake Mohave range.

The Large Area Calibration Pads (LACP) in Grand Junction, CO allow AMS to validate against known concentrations of K, U, and Th. Known quantities of K, U, and Th are measured from the pads and calibration factors are determined from the spectral regions of ^{40}K (1.46 MeV), and prominent daughters of ^{238}U (1.764 MeV), and ^{232}Th (2.642 MeV).

There are two methods that can be used to derive estimates for the concentrations of K, eU, and eTh from spectra. The first method is outlined in detail in a publication by the International Atomic Energy Agency (IAEA) [4]; in this report the method is referred to as the IAEA method. The IAEA method involves building a matrix of sensitivities to account for down scattering in K, and U window regions. The major disadvantage to the IAEA method is that the matrix is inflexible to the introduction of variable isotope mixes. The preferred AMS method involves fitting a Gaussian function to the primary photo-peaks of interest to extract counts above the continuum in each of those windows. A count to concentration coefficient is then determined for each spectral region. This report will refer to the method as the Gaussian method. Both methods produce statistically overlapping results within one standard deviation [6] & [8].

Before the spectra were analyzed for the extraction of element concentrations, a principle component analysis in the form of Noise Adjusted Single Value Decomposition (NASVD), was performed to reduce high level noise in the spectra [10] & [11]. The counts in each region of interest were then corrected for non-terrestrial background by subtraction of data acquired over an adjacent body of water according to Section 3.4. Finally, the data were height corrected to the ground level using the attenuation relationship.

In addition to the whole spectrum method used to determine exposure rate, an estimate can be made of the exposure contribution from K, eU, and eTh that, when summed, will approximately equal the total terrestrial exposure rate [7]. This allows for the calculation of exposure rate attributable to a specific element (e.g. exposure rate due to U). Table 4 highlights several published conversion factors for this analysis. Factors reported by Haber et. al. (2017) were used to determine exposure rate due to U.

Environmental radiation sources

Approximately 87 out of the 339 naturally occurring nuclides on Earth are unstable or radioactive. All minerals contain some degree of NORM. Cosmic rays, or highly energetic particles originating outside Earth's atmosphere, generate secondary forms of radiation

Table 4: Exposure rate from concentration conversion coefficient

Reference	μR/h per K(Wt%)	μR/h per eU(ppm)	μR/h per eTh(ppm)
Beck et al. (1972)	1.49	0.62	0.31
Løvborg and Kirkegaard (1974)	1.52	0.63	0.31
Haber (2017) [7]	1.24	0.41	0.22
AMS* (2019)	1.51	0.65	0.29

*Empirically determined from comparison of least square fit for concentrations and exposure on the pads.

including neutrons and gamma rays. Cosmic radiation levels vary as a function of latitude and altitude and range from 3μR/hr to 10μR/hr at 9000 ft above mean sea level (MSL) [1]. For the purpose of environmental monitoring, the radionuclies in the uranium and thorium (specifically ^{238}U and ^{232}Th) decay series are considered the most important [3]. Natural radiation that is aggregated through human intervention is referred to as technologically-enhanced NORM (TENORM) which is an industrial waste or byproduct containing naturally occurring radioactive elements found at higher levels than expected in the surrounding natural environment. It is possible that mining operations lead to residual TENORM. A primary objective of this report is to identify possible excess terrestrial levels of U to indicate potential areas for remediation from the DRUM sites.

Both the IAEA and Gaussian extraction methods, described in Section 3.2, generate U concentration estimates based on counts from gamma rays near 1765 keV emitted from ^{214}Bi. Thorium (^{232}Th) and Potassium (^{40}K) concentration estimates are based on decay chains and can be assumed to be in equilibrium to a high degree of accuracy. Thorium concentrations are estimated based on counts from gamma rays emitted near 2614 keV corresponding to emission from Thallium-208 (^{208}Tl), and ^{40}K estimates are based directly on emission of the 1461 keV photon. The estimates of U concentration are usually reported as eU as these estimates are also based on the assumption of secular equilibrium conditions. However ^{214}Bi, the great-granddaughter of ^{222}Rn is generated far in the radioactive decay chain and are not likely to be in perfect secular equilibrium with ^{238}U as in-growth of ^{226}Ra occurs on the order of 1000s of years. The relationship between ^{226}Ra and its daughter ^{222}Rn is a complex. Naturally a small proportion of radon diffuses from a depth of a few meters into the air. It is generally accepted that radon escapes from a particle as a result of recoil as ^{226}Ra decays. If the recoil terminates in an open pore, the radon is able to migrate. However, the recoil

range in solids is short, and most of the recoiling atoms are retained in the original particle. Because of this, at depth in soil ^{222}Rn and ^{226}Ra remain close to secular equilibrium. U is extracted from its ores by the sulphuric acid or the alkaline carbonate leaching process. The U content of most ores is low (0.08–3% U) and the bulk of the ore is rejected as mill-waste or tailings after U leaching. The daughter radionuclides of ^{238}U largely remain in place during U leaching. Therefore, almost all the radium initially present in the ore ends up in the mill tailings [12]. This implies that eU estimates from ponds and waste piles may overestimate U concentrations. However, as the bulk of gamma emissions from the U series are from its progeny, estimates of terrestrial exposure from aerial measurements using the extraction methods will be consistent with ground truth exposure rate measurements.

Airborne background correction

Uncorrected aerial gamma radiation measurements will include contributions from other radiation sources in the environment such as airborne radon, cosmic rays, and from contributions of naturally occurring radiation in the aircraft and crew. Therefore, in processing aerial gamma data a correction for non-terrestrial sources is vital.

Survey airborne background data were collected over the Pathfinder Reservoir or at high altitude (3000 ft AGL) in route to the survey area. It is important to note that the non-terrestrial background estimate would include radon. However, freshly diffused radon in the survey vicinity may account for some of the contributions to the ^{214}Bi lines not accounted for in a water line background or high altitude line. Counts due to local radon would therefore have a weighted impact on the count rate indicating a higher average U concentration then may be present. A minimum of two water lines flights were collected for each survey day, and high altitude lines were performed every flight in route to and from the survey area.

Quality Assurance/Quality Control

Pre-flight checks and NaI detector calibration

It is standard procedure for AMS to collect pre-flight data prior to a survey flight. At the start of each day diagnostic data was collected to evaluate the health of the detection system, quality of the data, and to assess whether there was an energy calibration drift. Pre-flight data collection consists of a 5-minute background measurement, and a 5-minute radiation source measurement. The radiation source consisted of two ^{137}Cs sources, placed one on each gamma pod, totaling approximately 10 μCi in activity. The aircraft radar altimeter

was tested each day using a set voltage input and response test, and the values of the radar altimeter are compared to the aircraft pressure altimeter in flight. System health and energy calibration was monitored continuously in flight. To maintain energy calibration in flight, the detector system is gain stabilized using the 1460.8 keV line associated with ^{40}K. At the end of each flight, one minute of data was collected on the ground and compared to the pre-flight data to ensure consistency from beginning to end.

Calibration, Validation, and Verification

Empirical terrestrial exposure calibration

Following a ground measurement campaign in 1995 [2], the Lake Mohave test lines (LMTL) have been used by AMS as an environmental reference standard to monitor and verify the integrity of AMS acquisition systems. The Lake Mohave calibration line (LMCL) is located approximately 0.6 mi (1 km) west of the western shoreline of Lake Mohave, Nevada, and 12.4 mi (20 km) east of Searchlight, Nevada. This calibration line is approximately 2.8 mi (4.6 km) long with elevation variations along the test line between 780 ft (240 m) to 960 ft (290 m) mean sea level (MSL). A second calibration flight line over Lake Mohave is referred to as the water line. This line is flown at the same altitude as the land line measurement for airborne background at a given altitude, and the data are used to correct for non-terrestrial background radiation. The calibration lines are depicted in Figure 9. The terrestrial NORM count exposure conversion coefficient and effective height attenuation coefficient are derived from repeated gamma radiation measurement flights over the land and water lines at Lake Mohave. The default count to exposure coefficient for background corrected (net) gamma counts on the energy window of 24 to 3066 keV is $3.2\text{e}^{-4}[(\mu R/hr)/cps]$. The default effective height attenuation coefficient for gamma counts in this range from an altitude of 50 to 1200 feet is 0.0017 ft^{-1}. In 2014, an aerial survey and ground survey were completed. As part of this campaign, physical soil and rock samples as well as ground measurements performed both with an HPGe detector and a PIC were acquired. The physical samples were counted in a gamma counting laboratory and also processed by inductively coupled plasma mass spectrometry (ICP-MS), yielding concentrations of K, U, and Th. The results validated the use of the LMCL for aerial measurement exposure rate calibration [8]. In addition, these results were validated against AMS measurements at the LACP in Grand Junction, Colorado. [6].

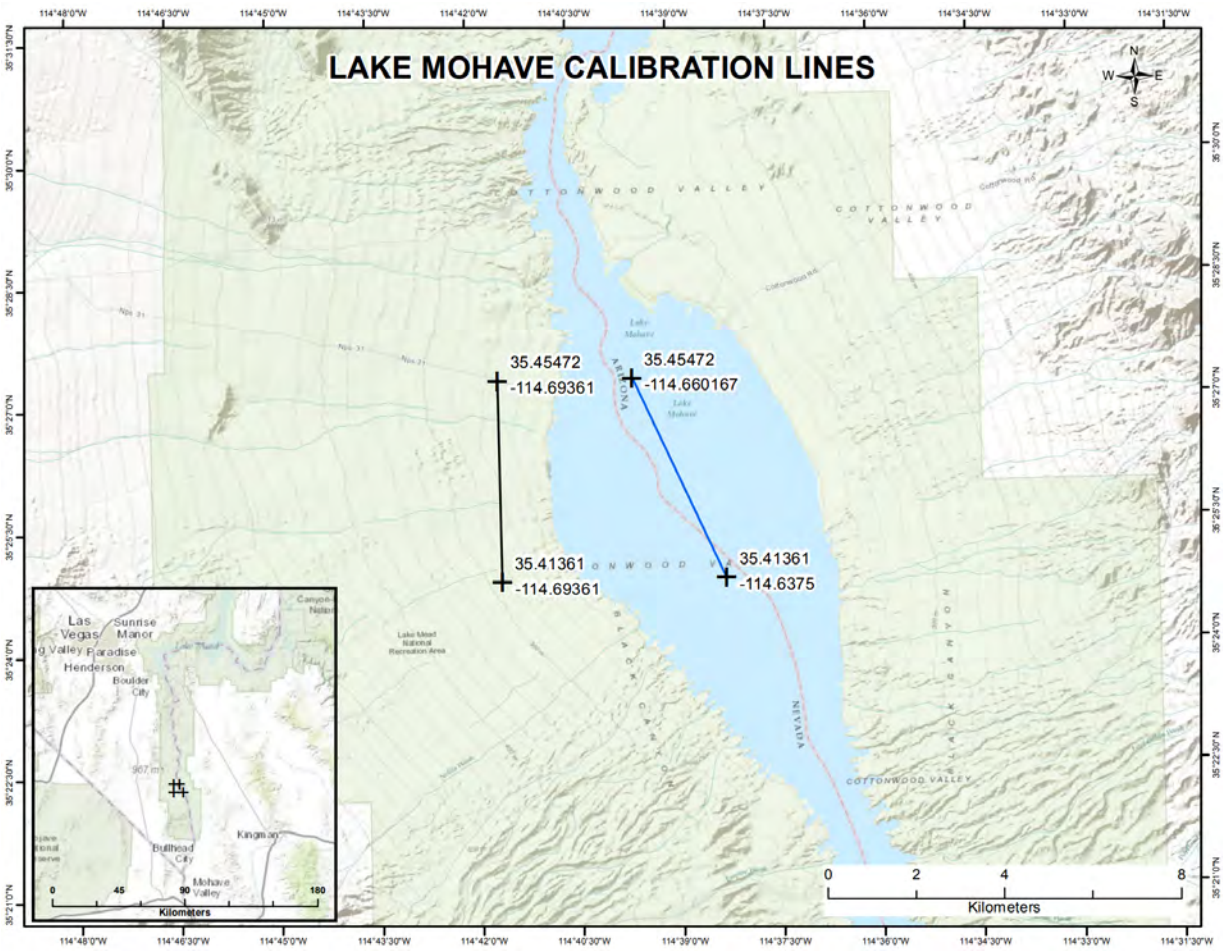

Figure 9: The Lake Mohave calibration lines.

Validation of aerial based terrestrial exposure measurements at Shirley Basin

The AMS estimates for exposure rate 1-m above ground have been validated by direct measurements for this survey campaign. The team performed in-situ PIC measurements at the Shirley Basin site on August 8, 2021. Each 5 minute PIC measurement was corrected for expected cosmic radiation which was determined as function of mean sea level and latitude [1]. There was no correction applied for local radon which could contribute anywhere from 0.25 to 5 μR/hr. The ground based measurements are compared to the raster averaged geo-located AMS measurements in Table 5 and Figure 11. For the fifteen measurement locations the average difference between the aerial exposure rate measurements and the PIC was less than 2 μR/hr with a max difference of 4.6 μR/hr at location 14. However, all measurements

(a) In-situ 1-m exposure rate measurement location example 1

(b) In-situ 1-m exposure rate measurement location example 2

Figure 10: In-situ pressurized ion chamber measurements at Shirley Basin

overlapped in terms of the uncertainty for each measurement at each location. Two examples of the PIC measurements are shown in Figure 10.

Table 5: Terrestrial exposure rate comparison from pressurized ion chamber and AMS measurements

Point	Latitude	Longitude	Exposure Rate μR/hr	
			PIC*	AMS†
1	42.3297	-106.214	10.6	9.3
2	42.3298	-106.210	9.3	9.3
3	42.3295	-106.208	12.3	9.3
4	42.3289	-106.206	13.6	9.8
5	42.3287	-106.204	12.0	9.6
6	42.3291	-106.200	12.1	12.4
7	42.3290	-106.197	12.5	13.6
8	42.3292	-106.194	16.5	13.7
9	42.3291	-106.191	16.9	13.0
10	42.3293	-106.188	23.1	20.9
11	42.3303	-106.184	22.6	19.9
12	42.3304	-106.183	20.2	16.8
13	42.3305	-106.181	21.8	17.2
14	42.3301	-106.180	15.5	15.1
15	42.3301	-106.178	13.8	13.4

*Pressurized ion chamber measurements corrected for cosmic contribution [$\sim$7.5 μR/hr], but not radon [0-5 μR/hr]

†AMS data pulled from raster values for terrestrial exposure rates

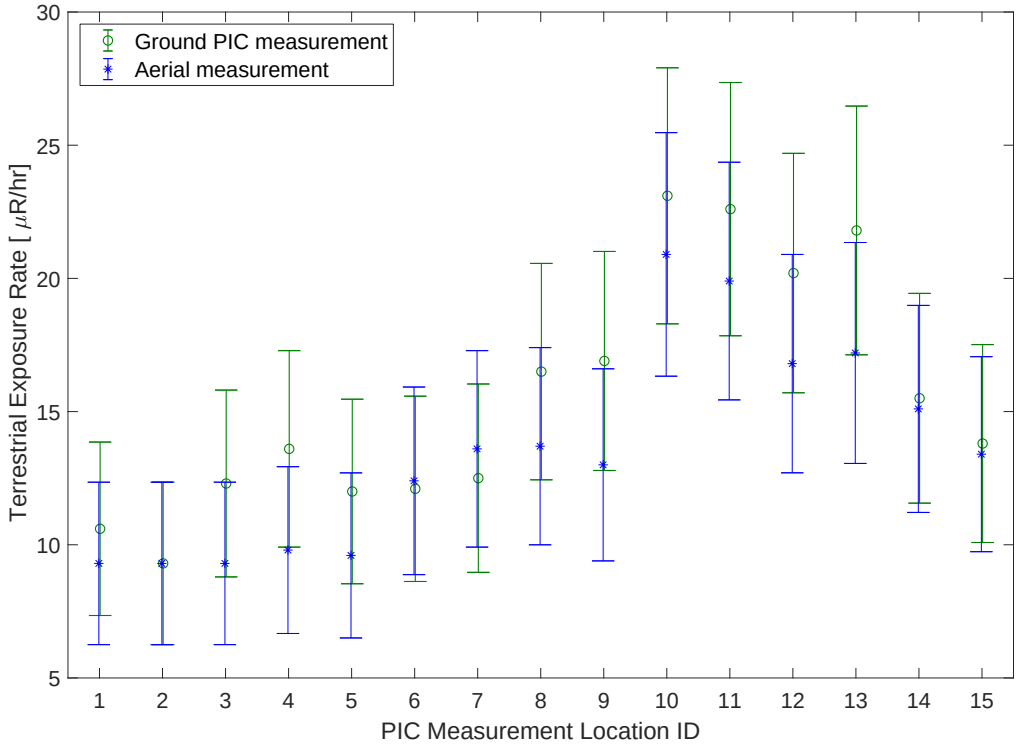

Figure 11: Pressurized ion chamber measurements corrected for a cosmic contribution of 7.5 μR/hr compared to raster values for AMS terrestrial exposure rate estimates at the same GPS location

Map Products and Results

Geographic information system data and results to accompany this report

The geographic information system (GIS) data were used to generate 6 maps per survey for a total of 18 maps comprised. All gamma data were collected as spectral data. Additional gamma spectral data files delivered with this report, and the list of map products is included in the list below:

- Uncorrected total gamma gross counts [cps] (files: geodatabase, kmls)
  - Shirley Basin uncorrected gamma gross counts [cps] Figure 12
  - Crooks Gap uncorrected gamma gross counts [cps] Figure 13
  - Gas Hills uncorrected gamma gross counts [cps] Figure 14

- Terrestrial gamma exposure rates in μR/hr (file: geodatabase, (GEO tiff), kmls)
  - Shirley Basin total terrestrial exposure Figure 15
  - Crooks Gap total terrestrial exposure Figure 16
  - Gas Hills total terrestrial exposure Figure 17
- Terrestrial exposure rate due to uranium μR/hr (file: geodatabase, (GEO tiff), kmls)
  - Shirley Basin exposure from uranium Figure 18
  - Crooks Gap exposure from uranium Figure 19
  - Gas Hills exposure from uranium Figure 20
- Uranium equivalent concentrations [ppm] (file: geodatabase, (GEO tiff), kmls)
  - Shirley Basin uranium equivalent concentrations Figure 21
  - Crooks Gap uranium equivalent concentrations Figure 22
  - Gas Hills uranium equivalent concentrations Figure 23
- Potassium concentrations [weight percent (Wt%)]
  - Shirley Basin potassium concentrations Figure 27
  - Crooks Gap potassium concentrations Figure 28
  - Gas Hills potassium concentrations Figure 29
- Thorium equivalent concentrations [ppm]
  - Shirley Basin thorium concentrations Figure 24
  - Crooks Gap thorium concentrations Figure 25
  - Gas Hills thorium concentrations Figure 26
- Spectral CSVs for each survey to include latitude, longitude, and radar altimeter data

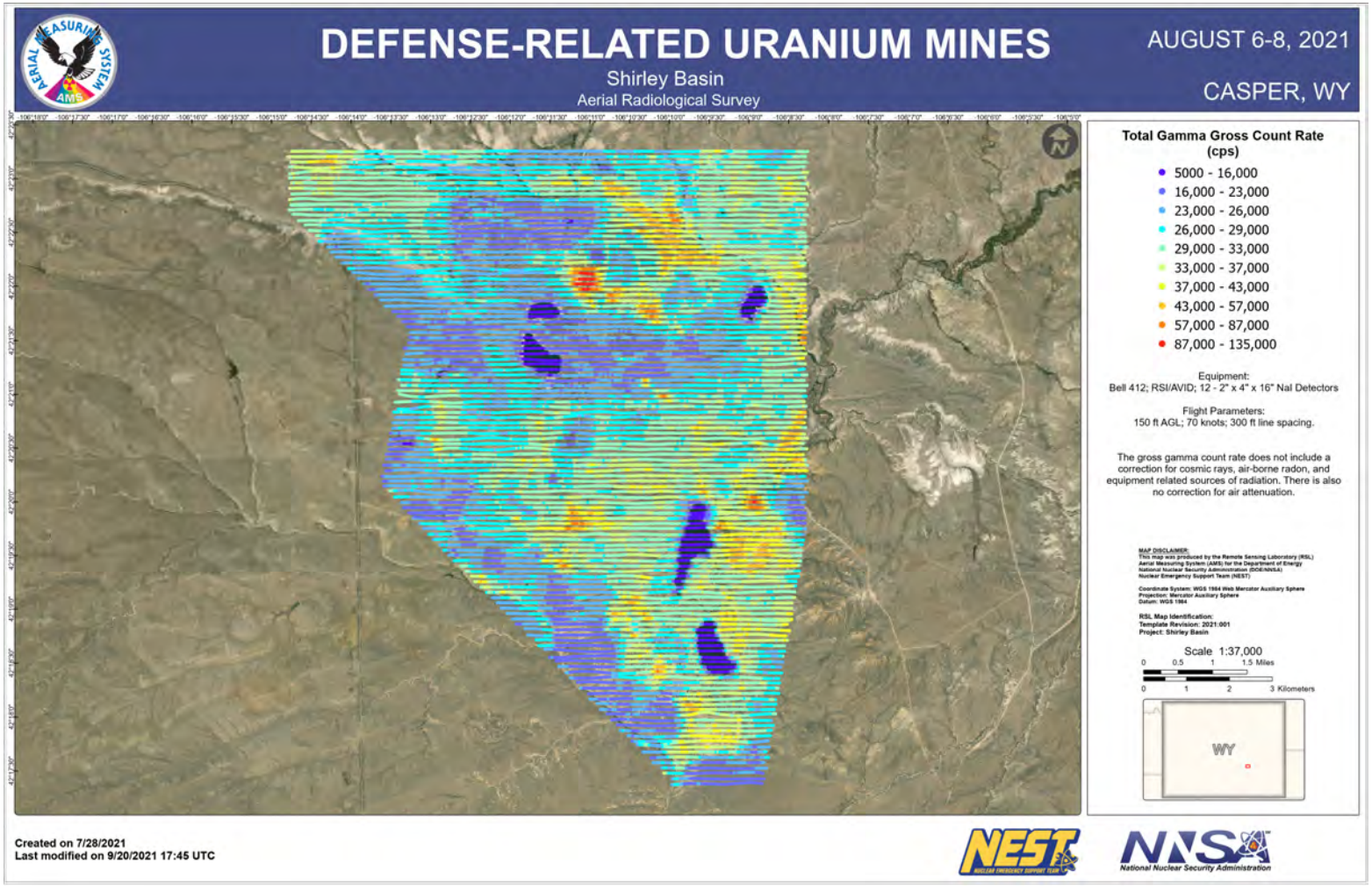

Figure 12: Total gamma gross count rate at Shirley Basin

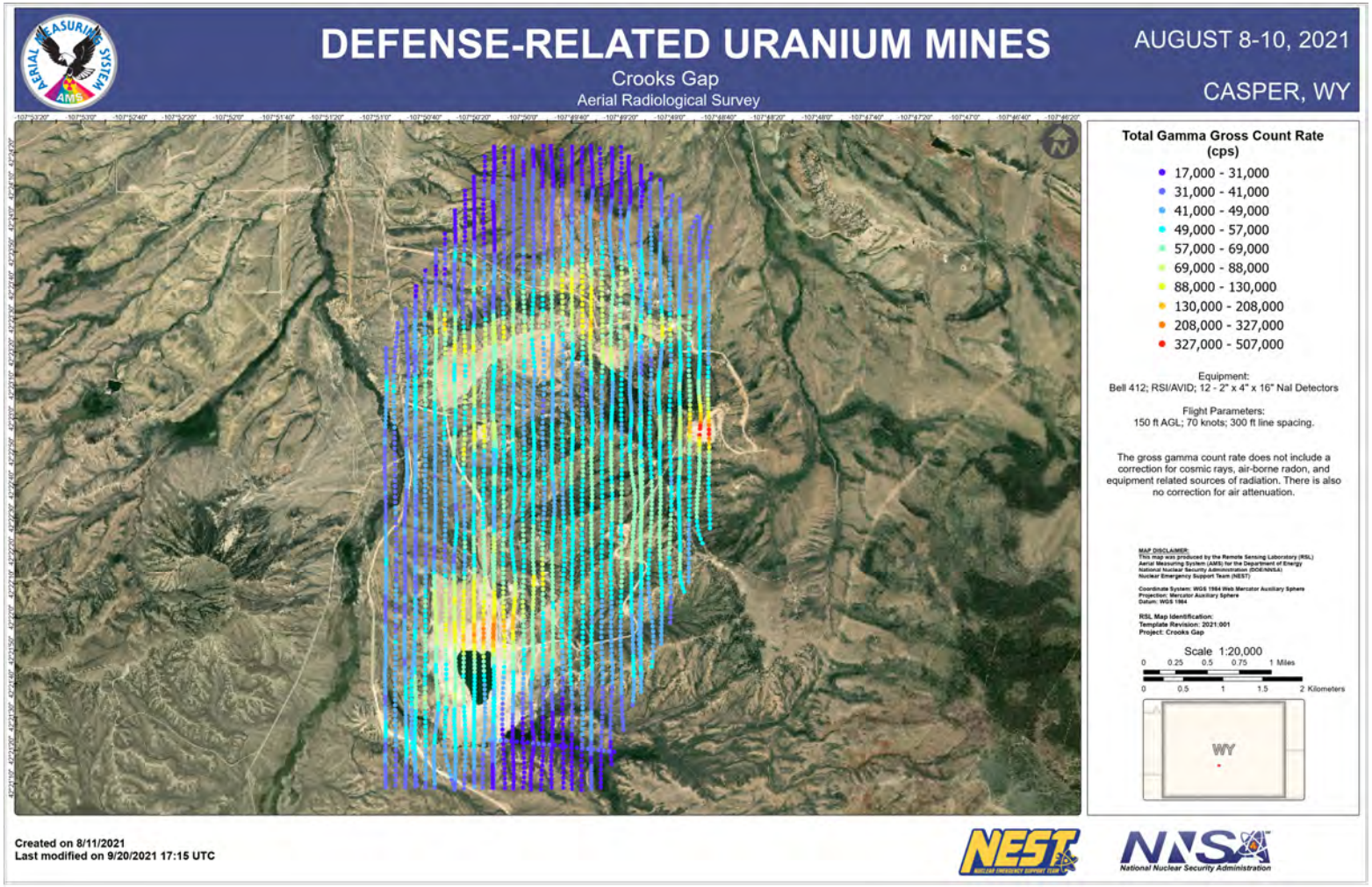

Figure 13: Total gamma gross count rate at Crooks Gap

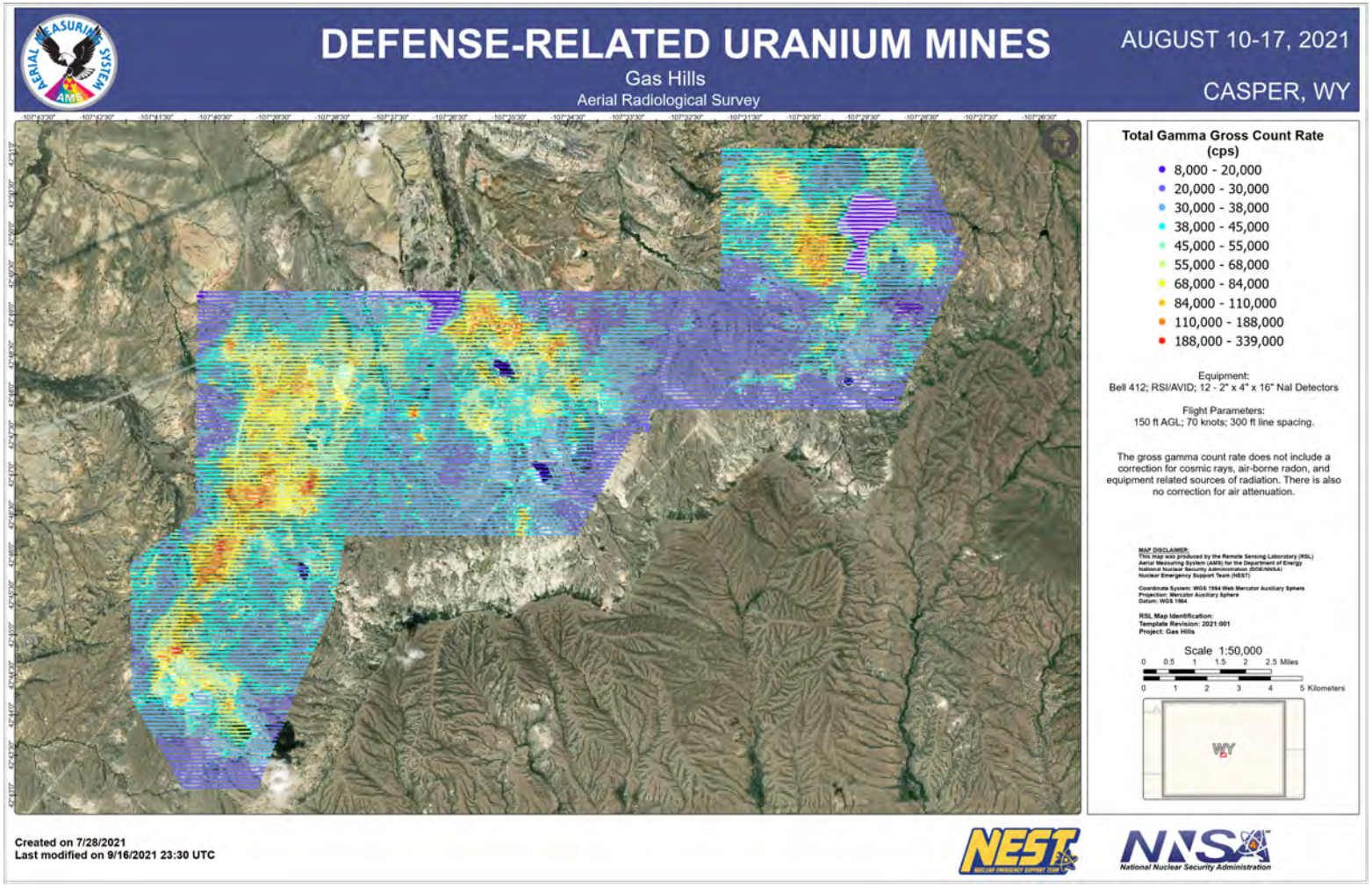

Figure 14: Total gamma gross count rate at Gas Hills

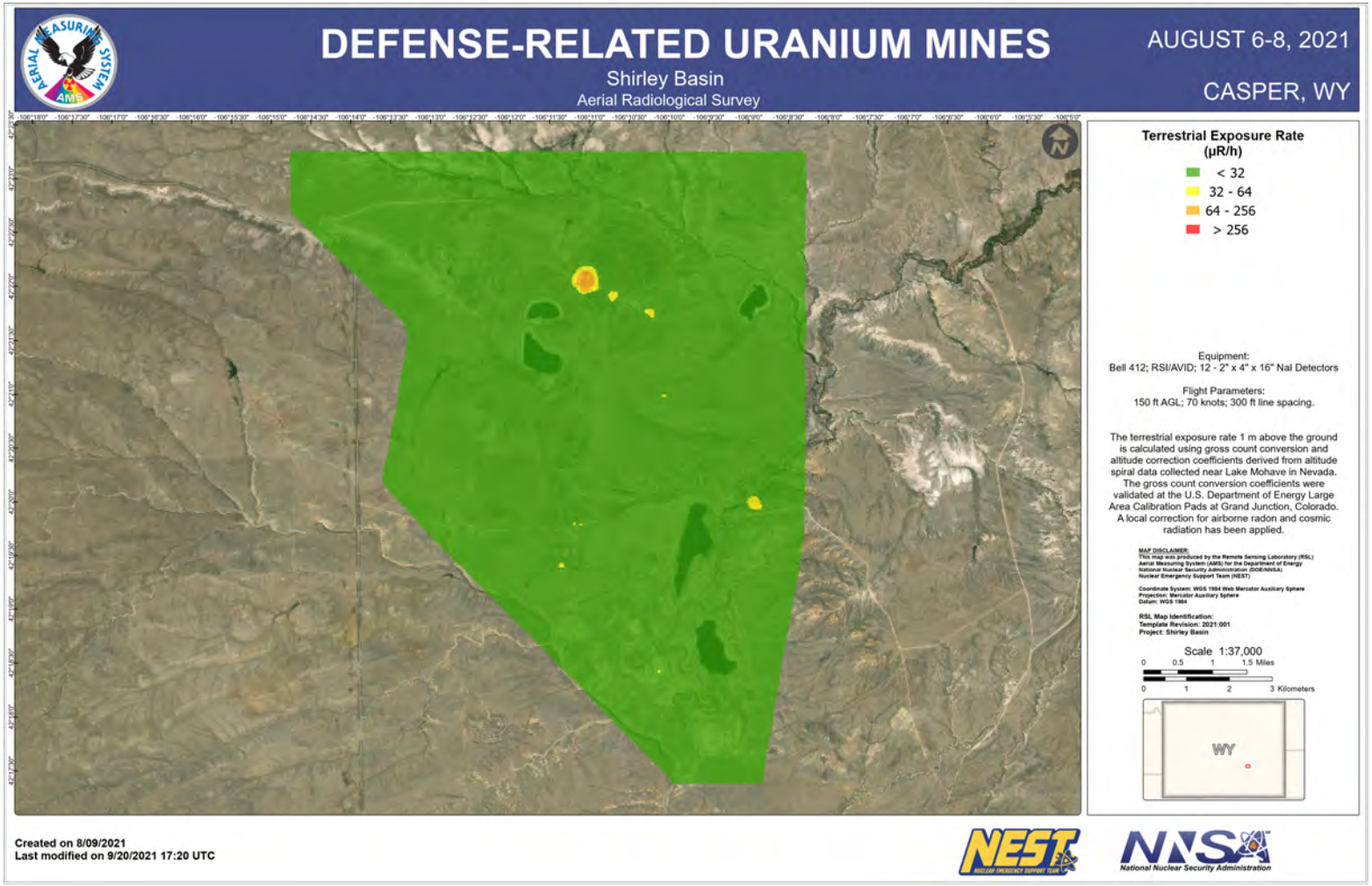

Figure 15: Total terrestrial exposure rate in μR/hr at Shirley Basin

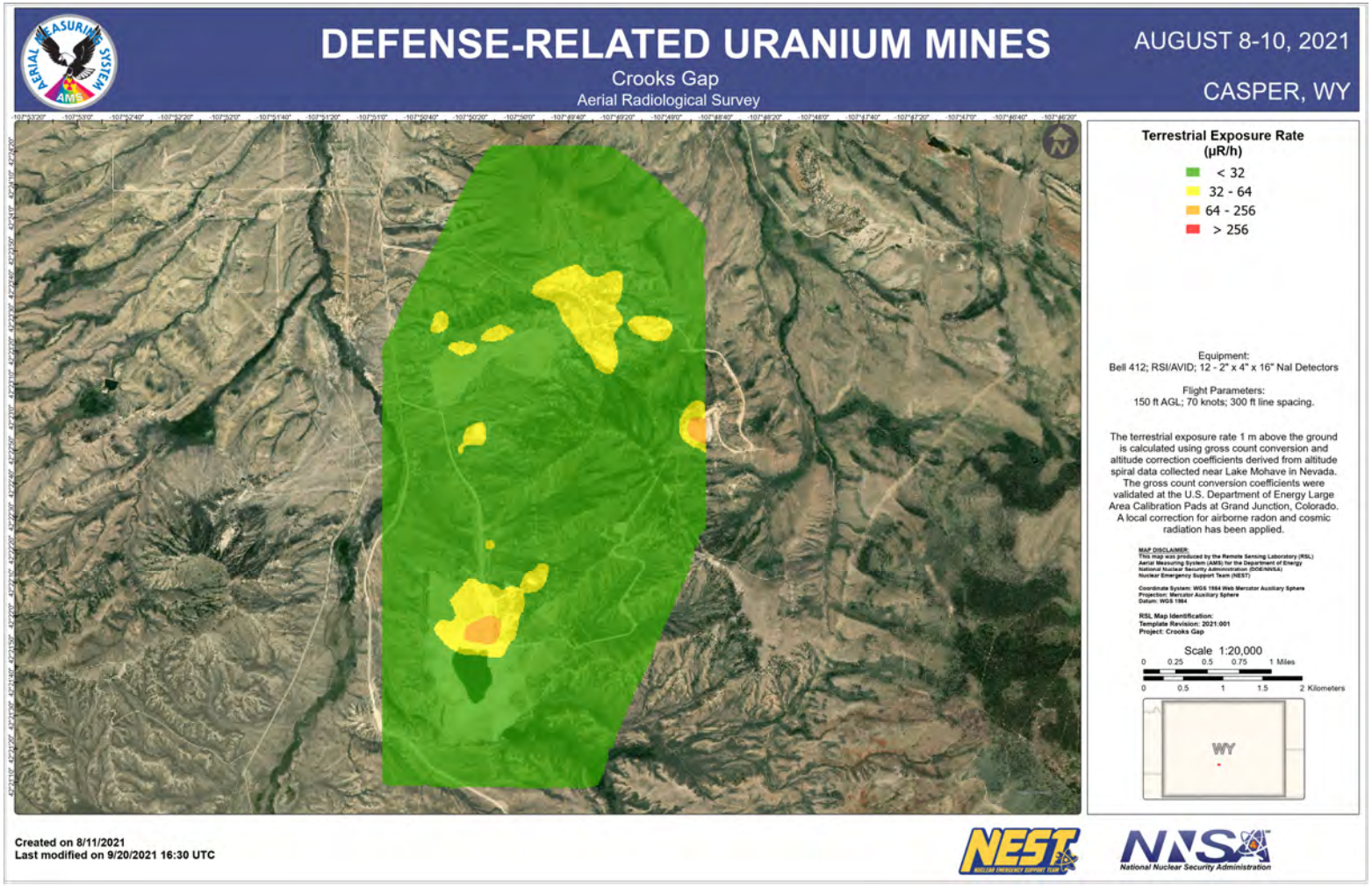

Figure 16: Total terrestrial exposure rate in μR/hr at Crooks Gap

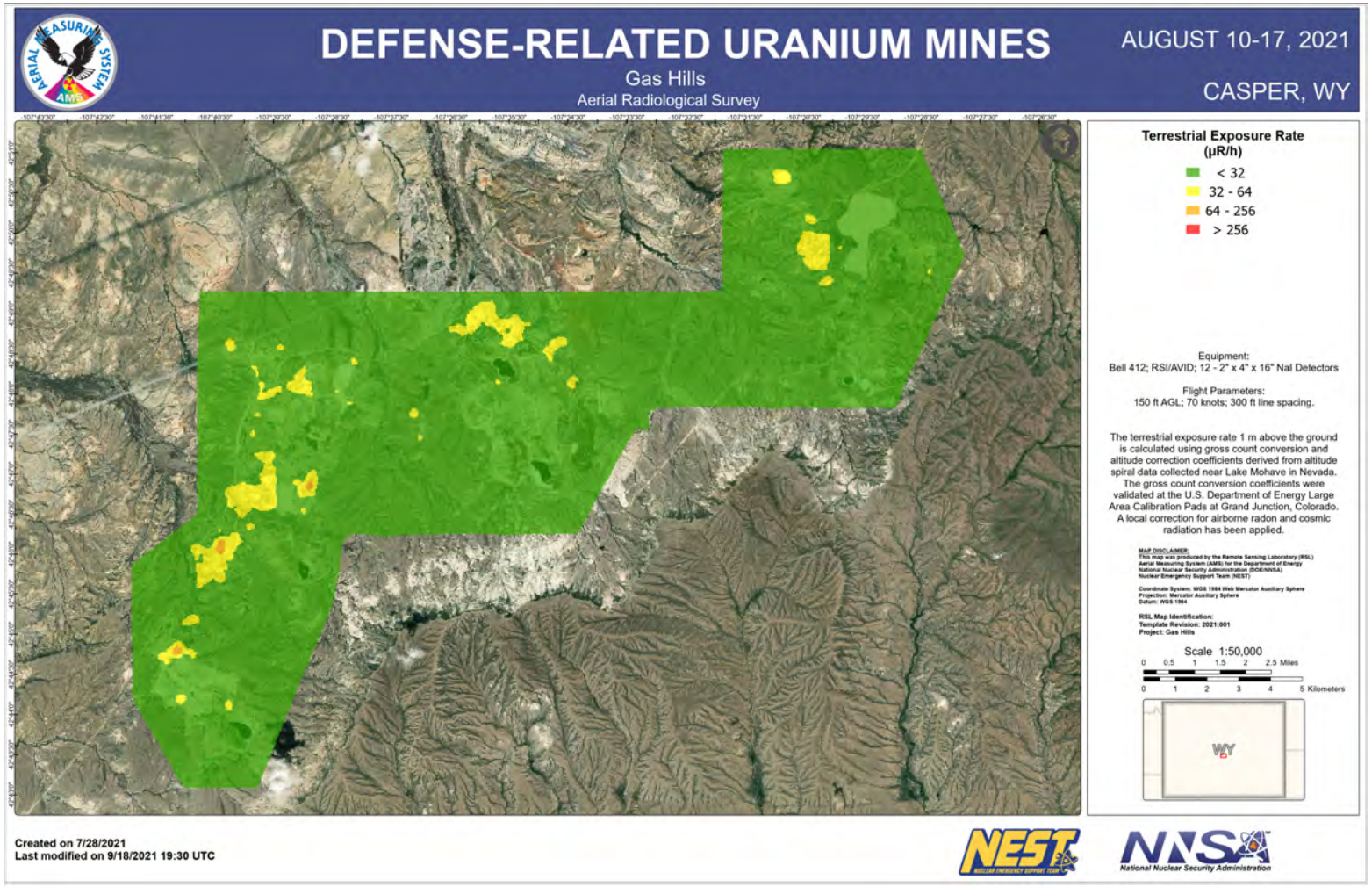

Figure 17: Total terrestrial exposure rate in μR/hr at Gas Hills

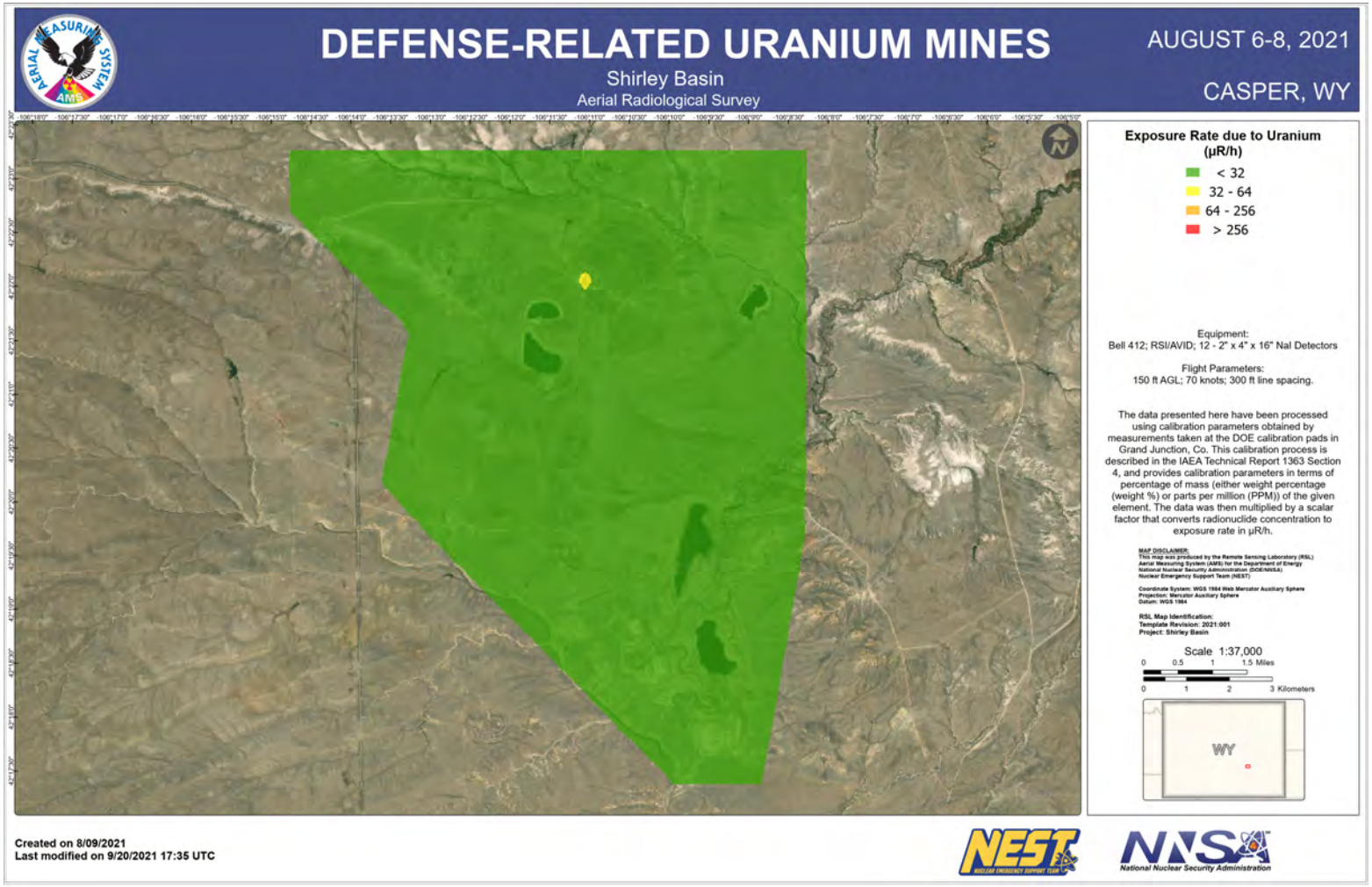

Figure 18: Exposure rate due to uranium in μR/hr at Shirley Basin

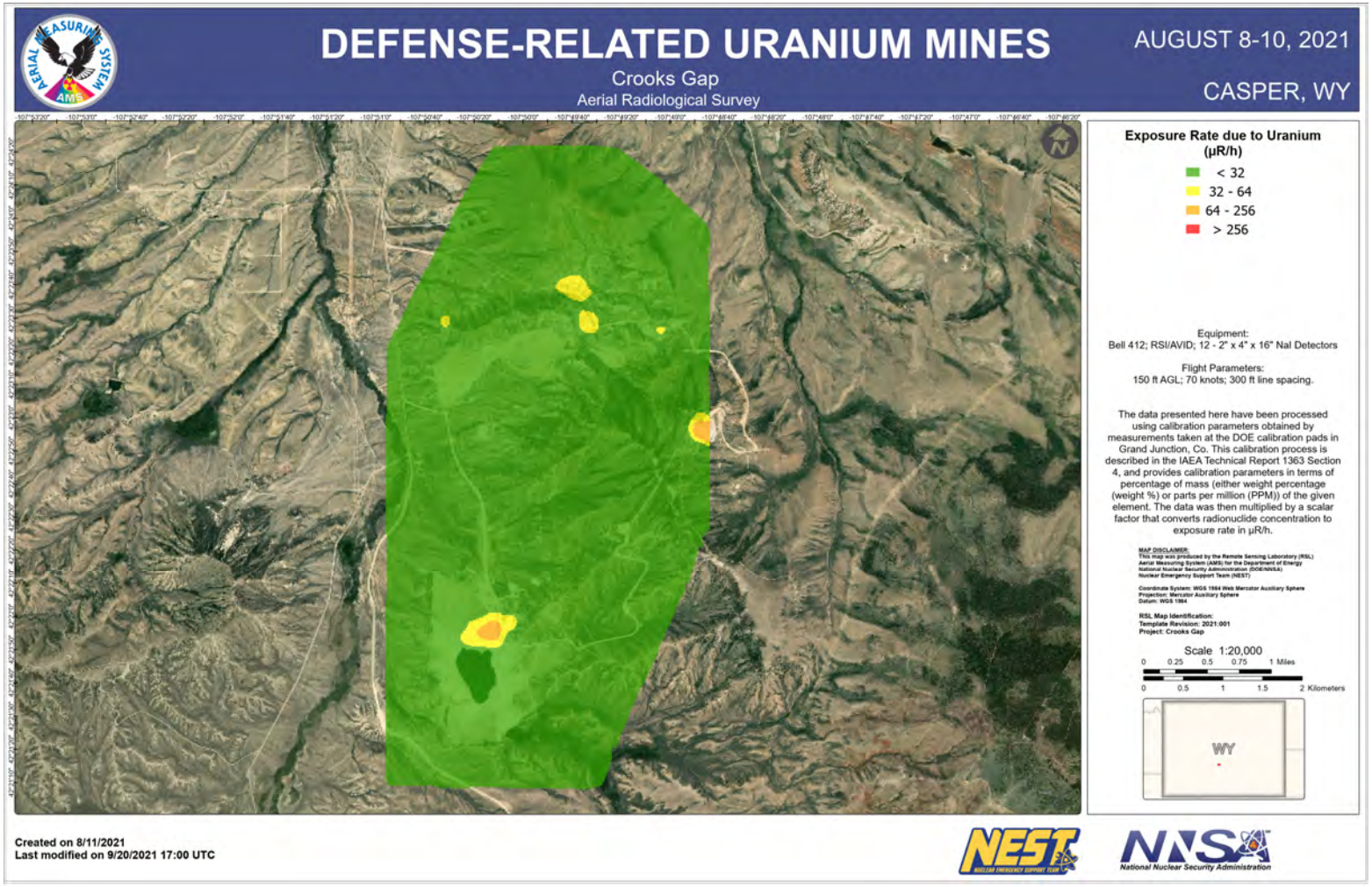

Figure 19: Exposure rate due to uranium in μR/hr at Crooks Gap

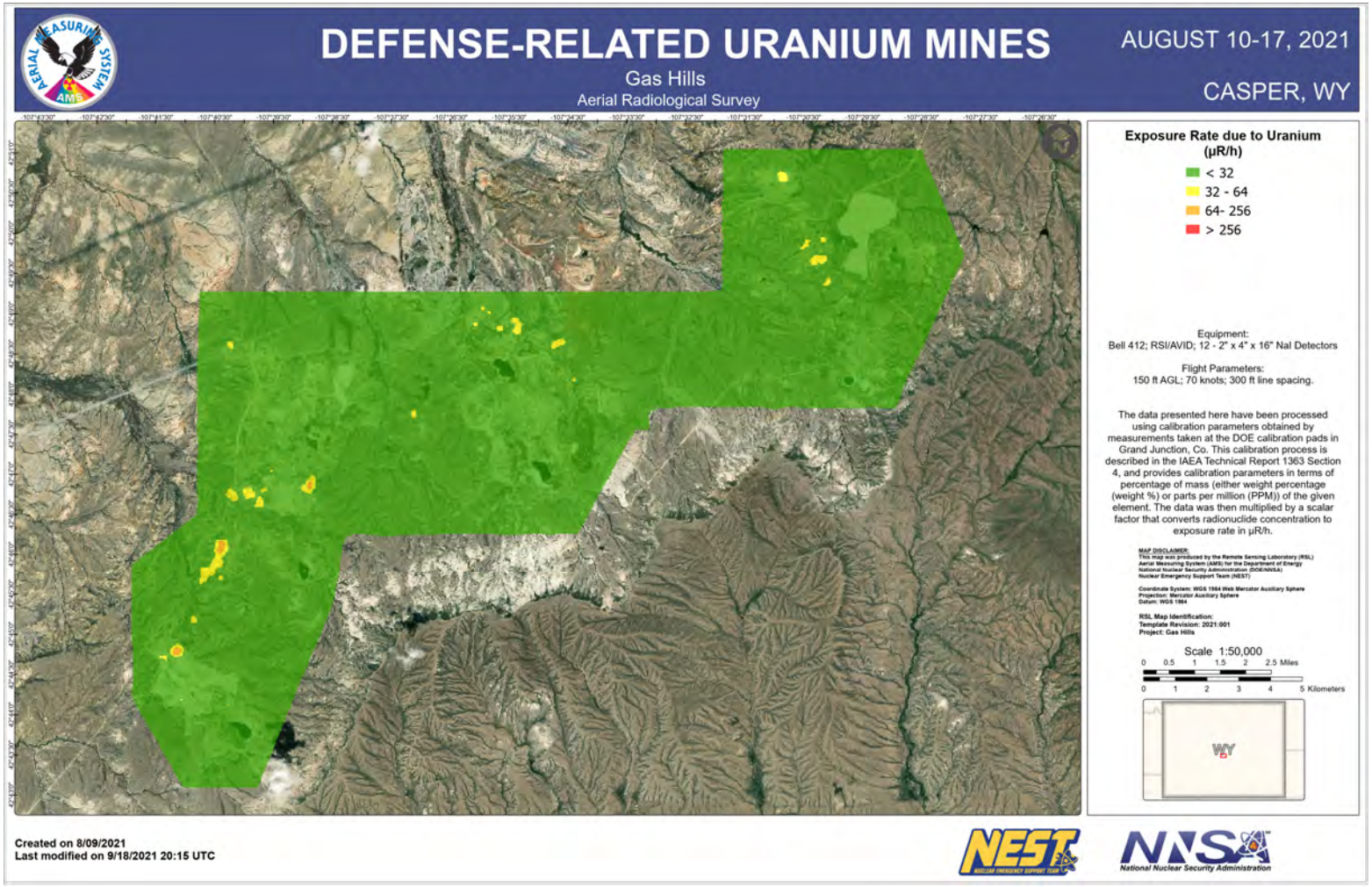

Figure 20: Exposure rate due to uranium in μR/hr at Gas Hills

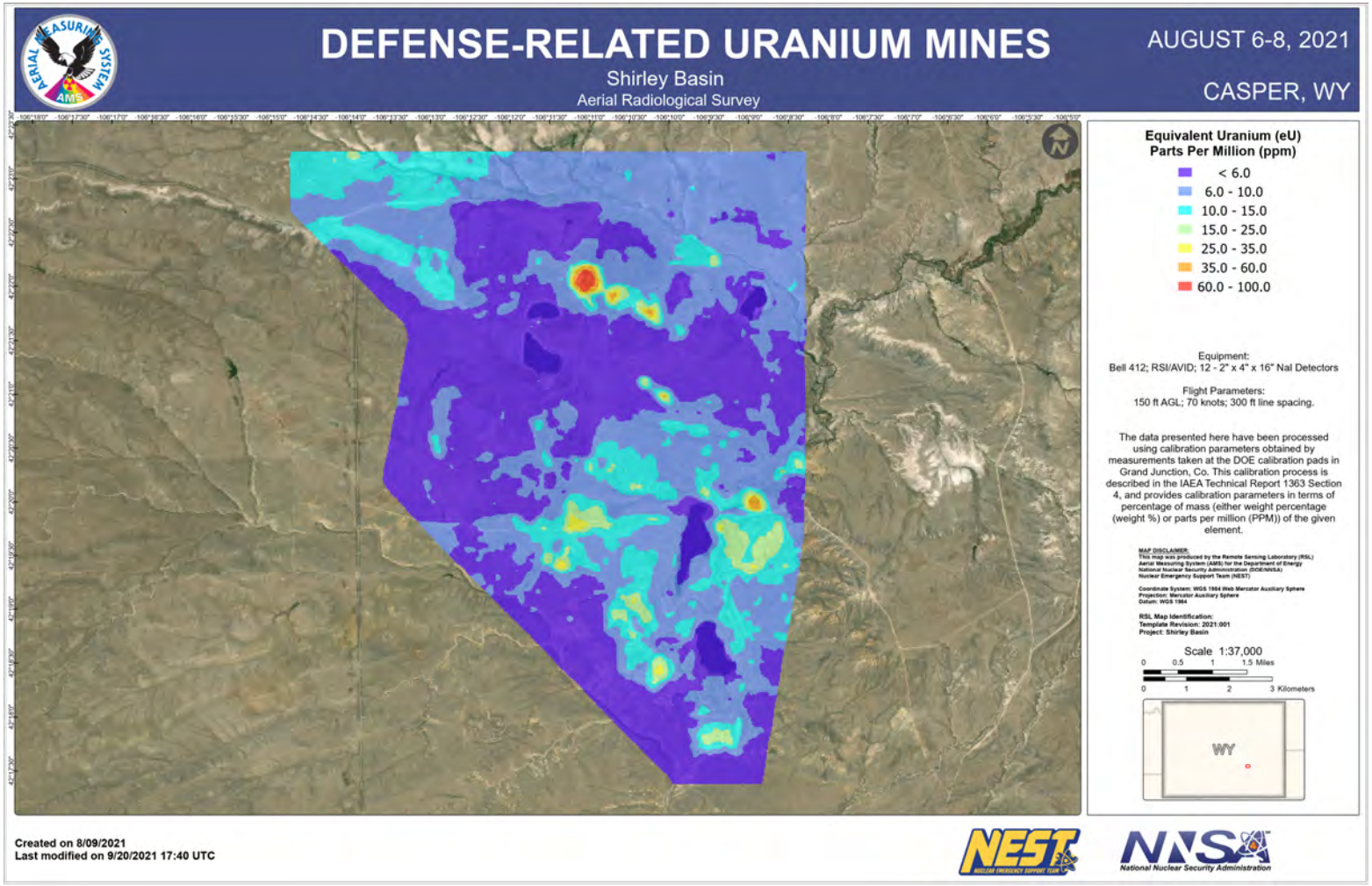

Figure 21: Equivalent uranium concentration results at Shirley Basin

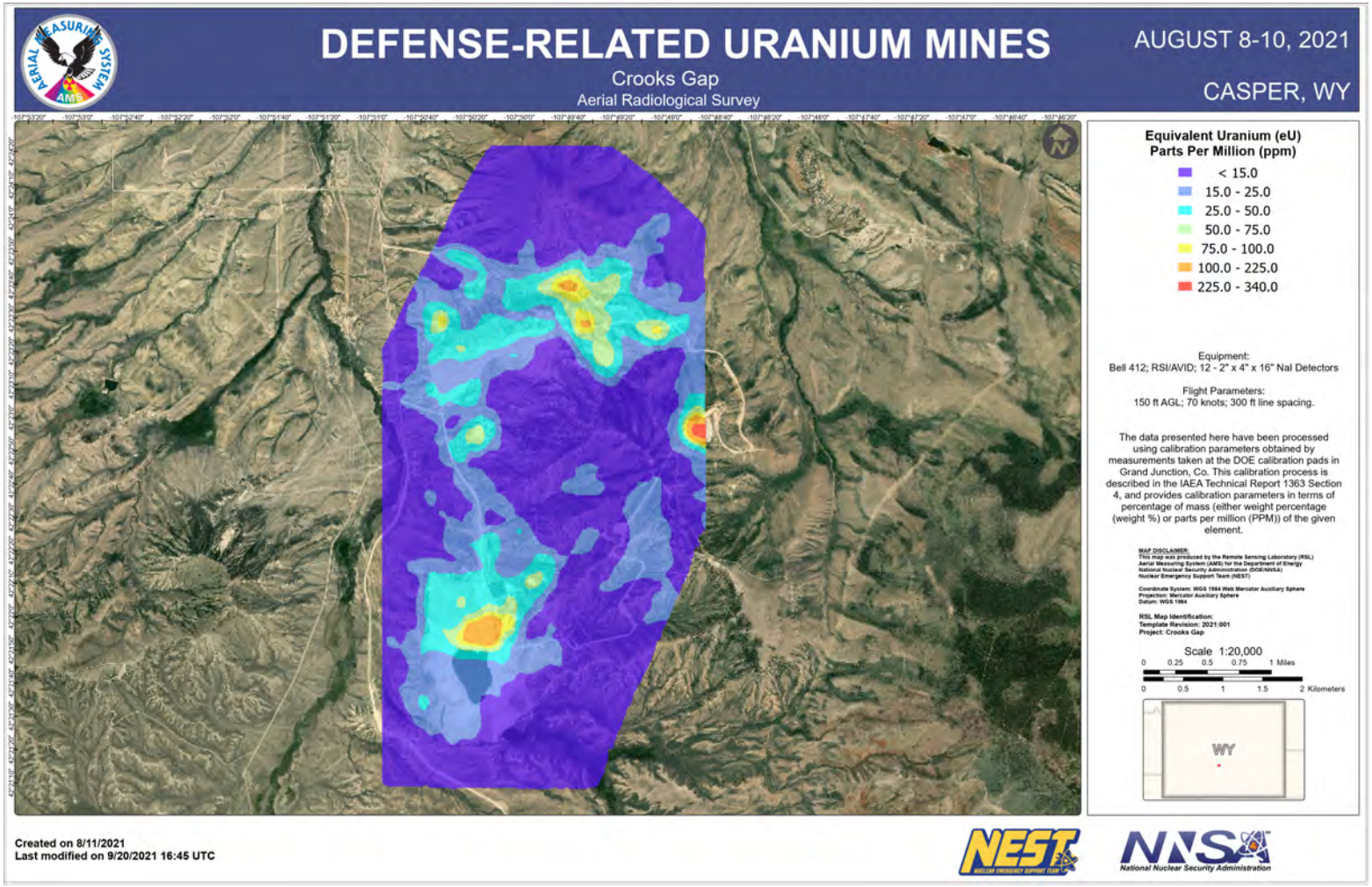

Figure 22: Equivalent uranium concentration results at Crooks Gap

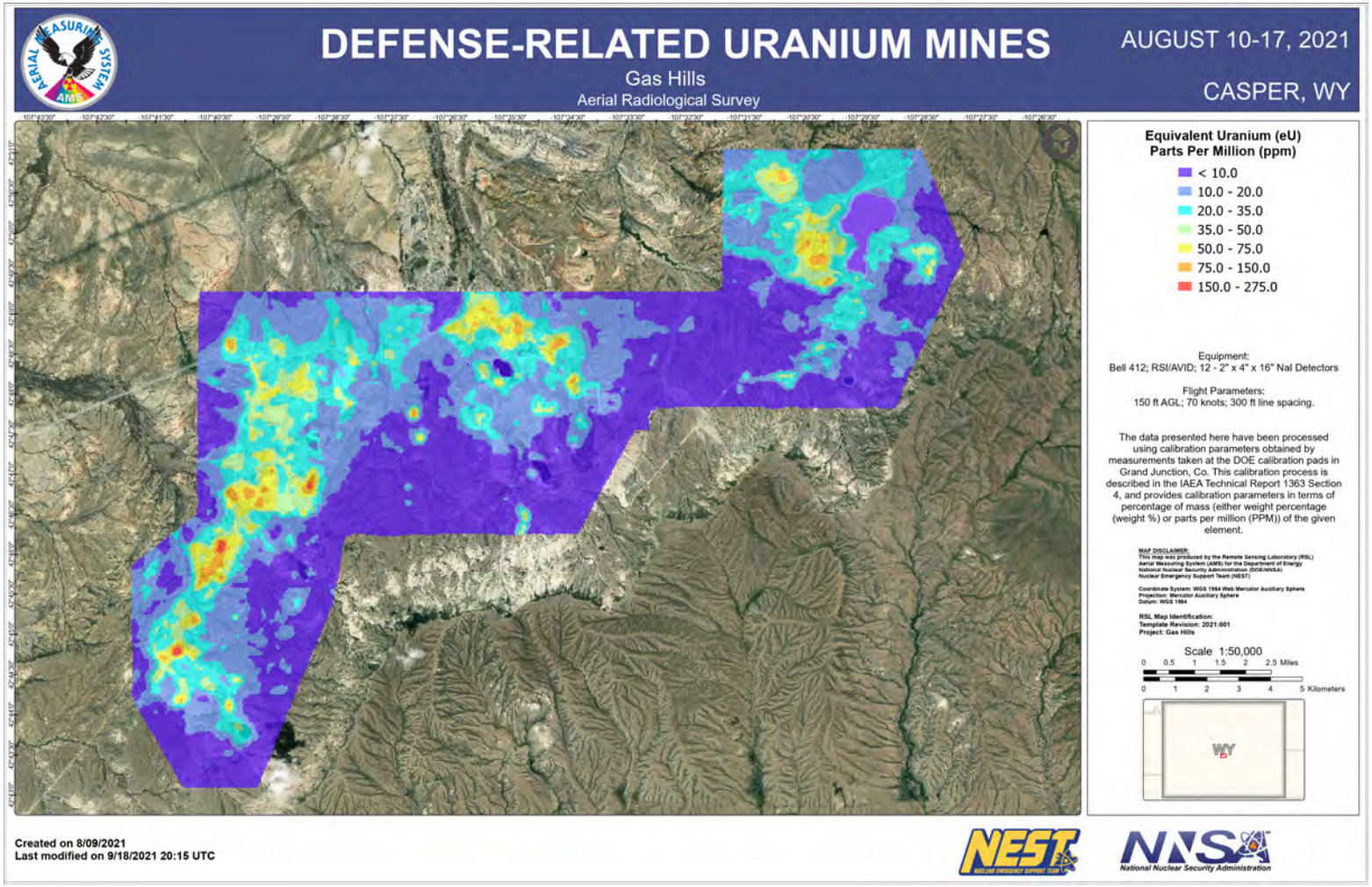

Figure 23: Equivalent uranium concentration results at Gas Hills

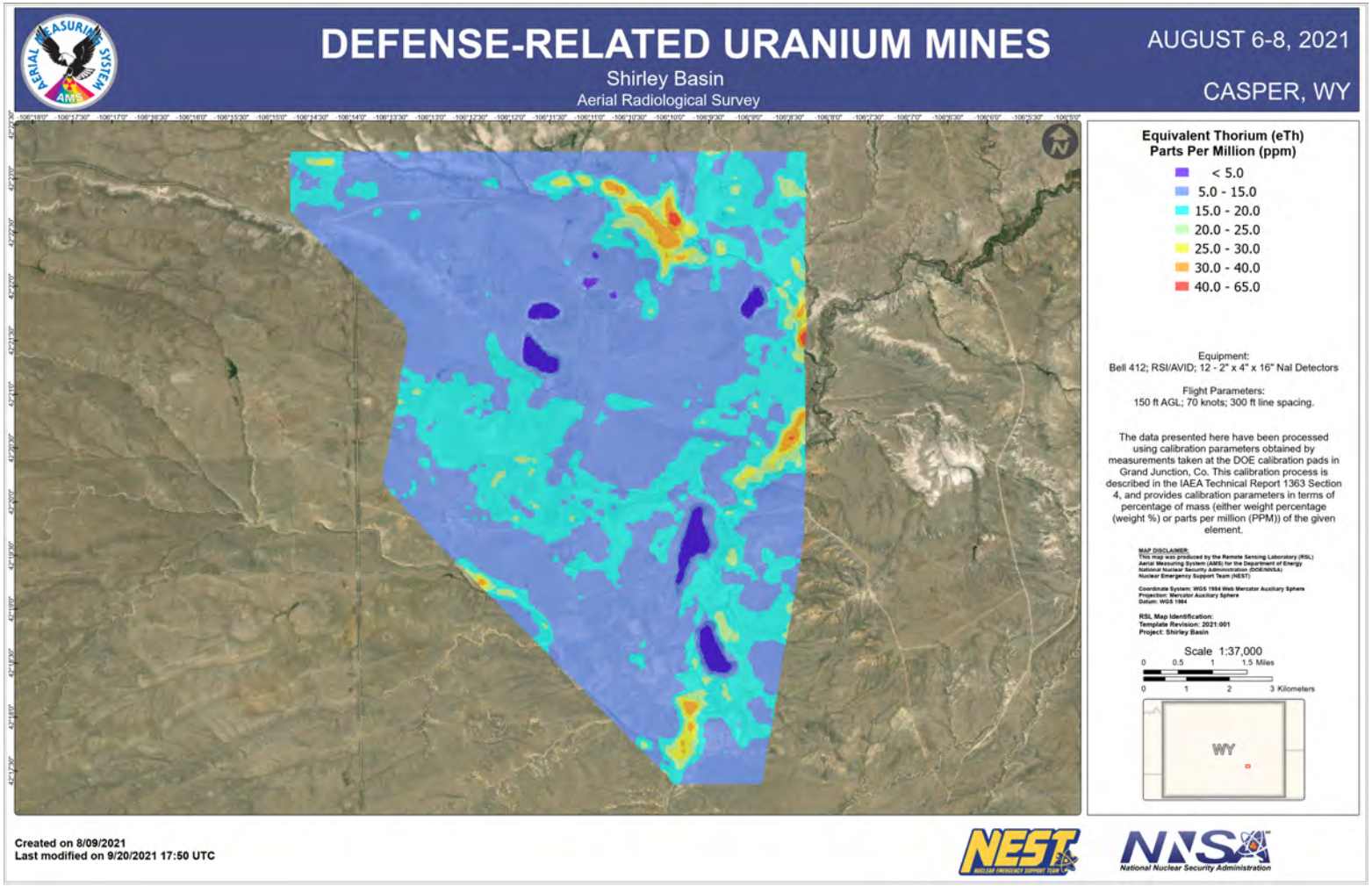

Figure 24: Equivalent thorium concentration results at Shirley Basin

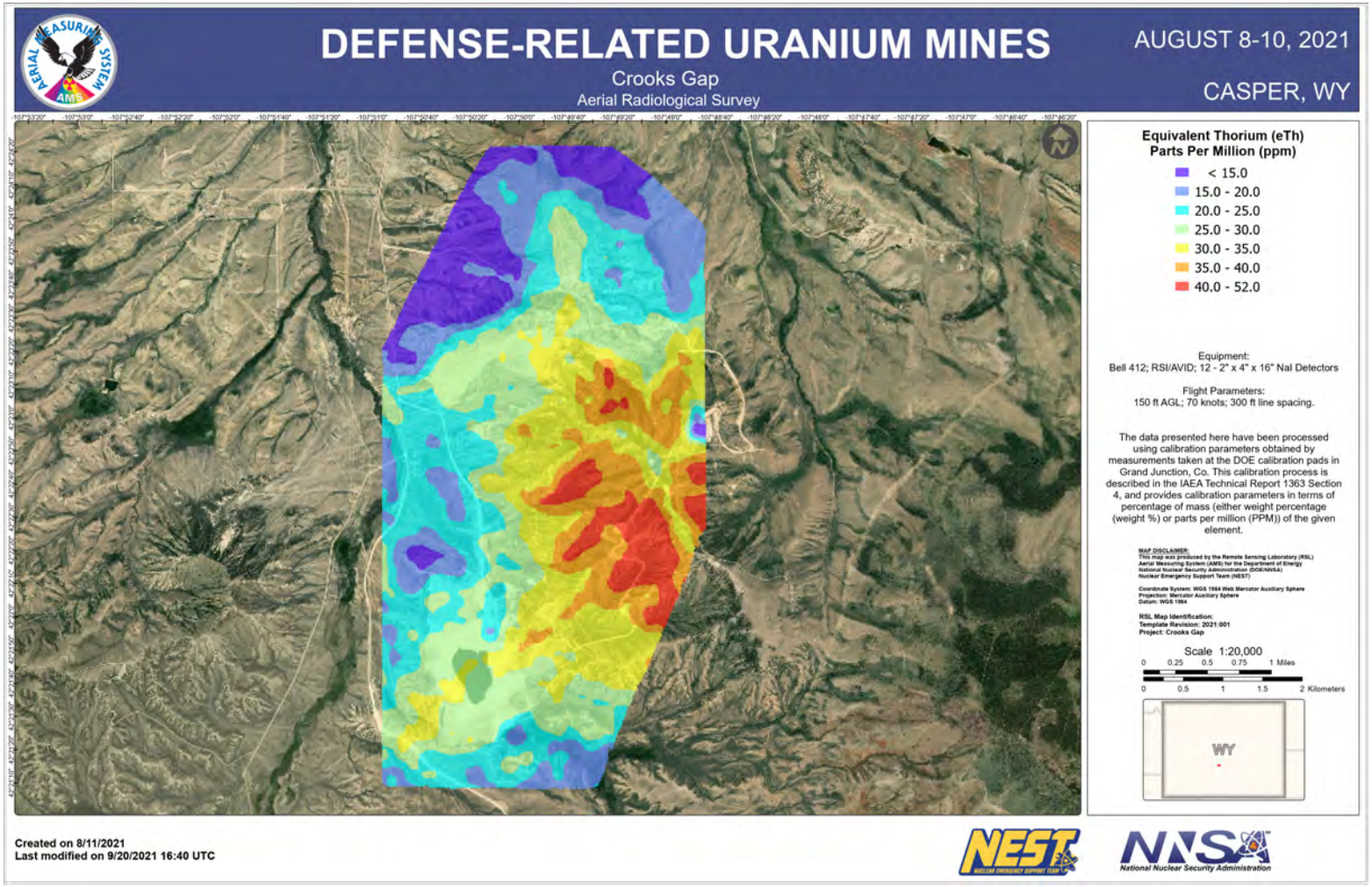

Figure 25: Equivalent thorium concentration results at Crooks Gap

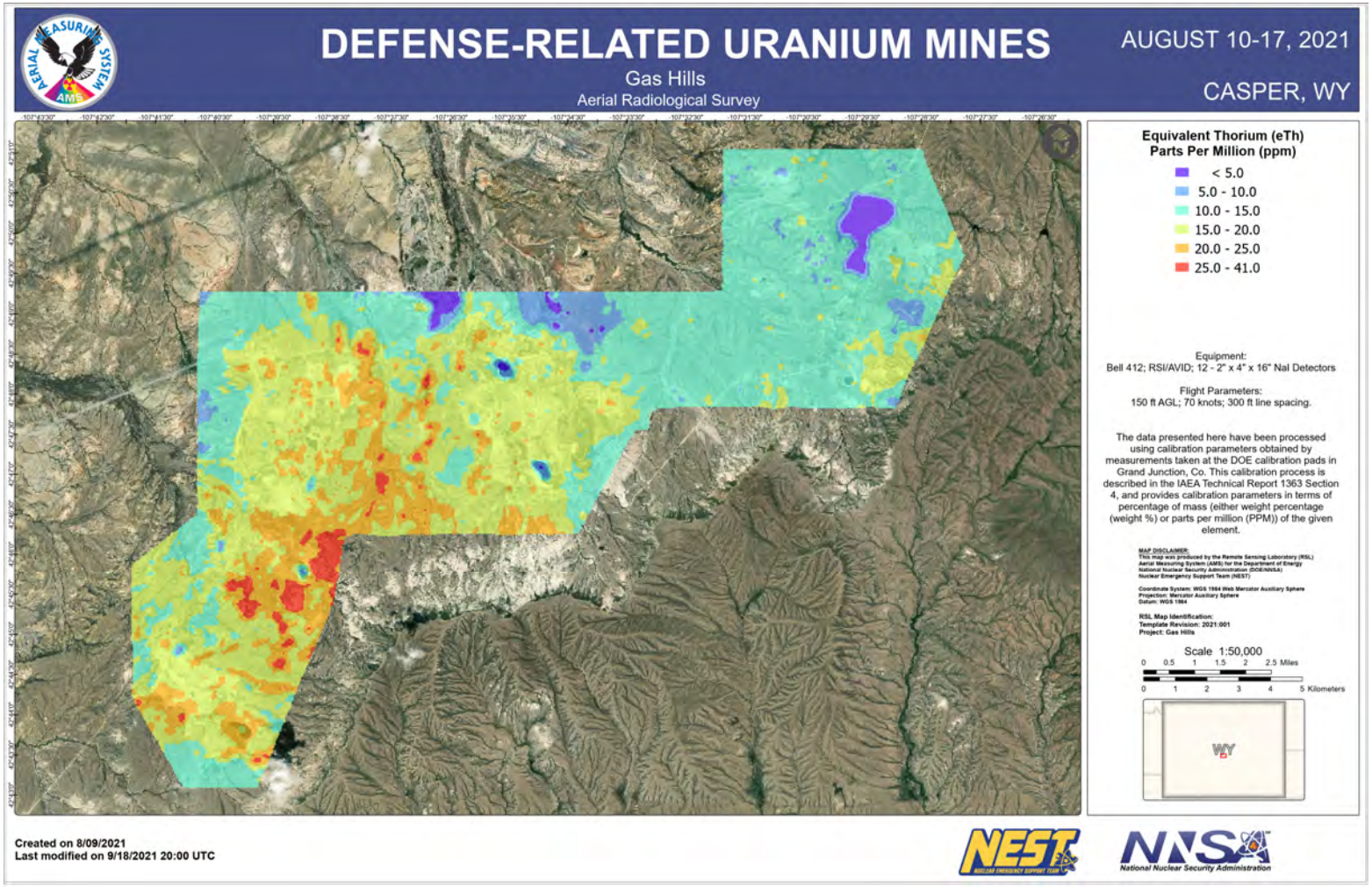

Figure 26: Equivalent thorium concentration results at Gas Hills

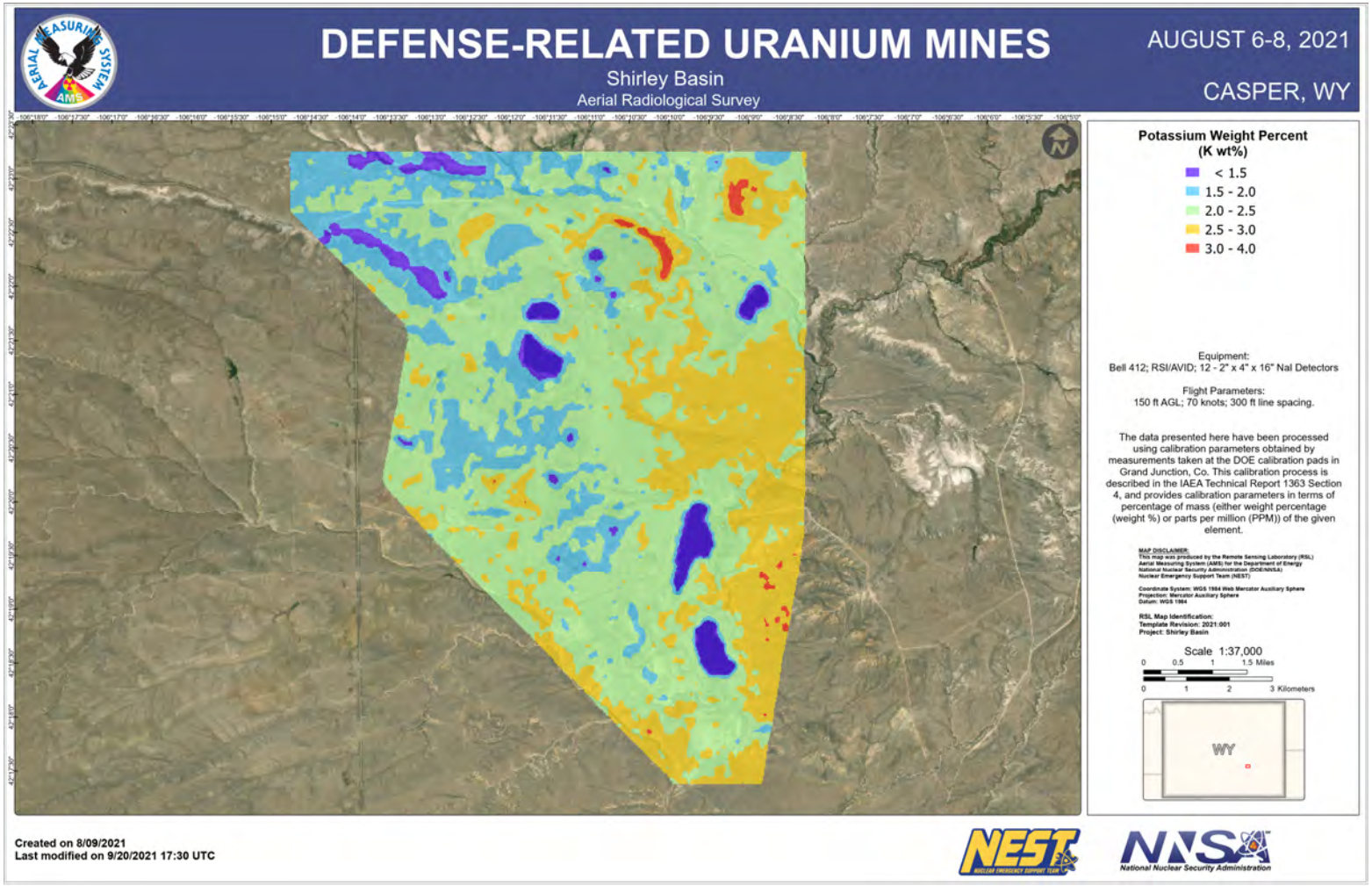

Figure 27: Potassium concentration results at Shirley Basin

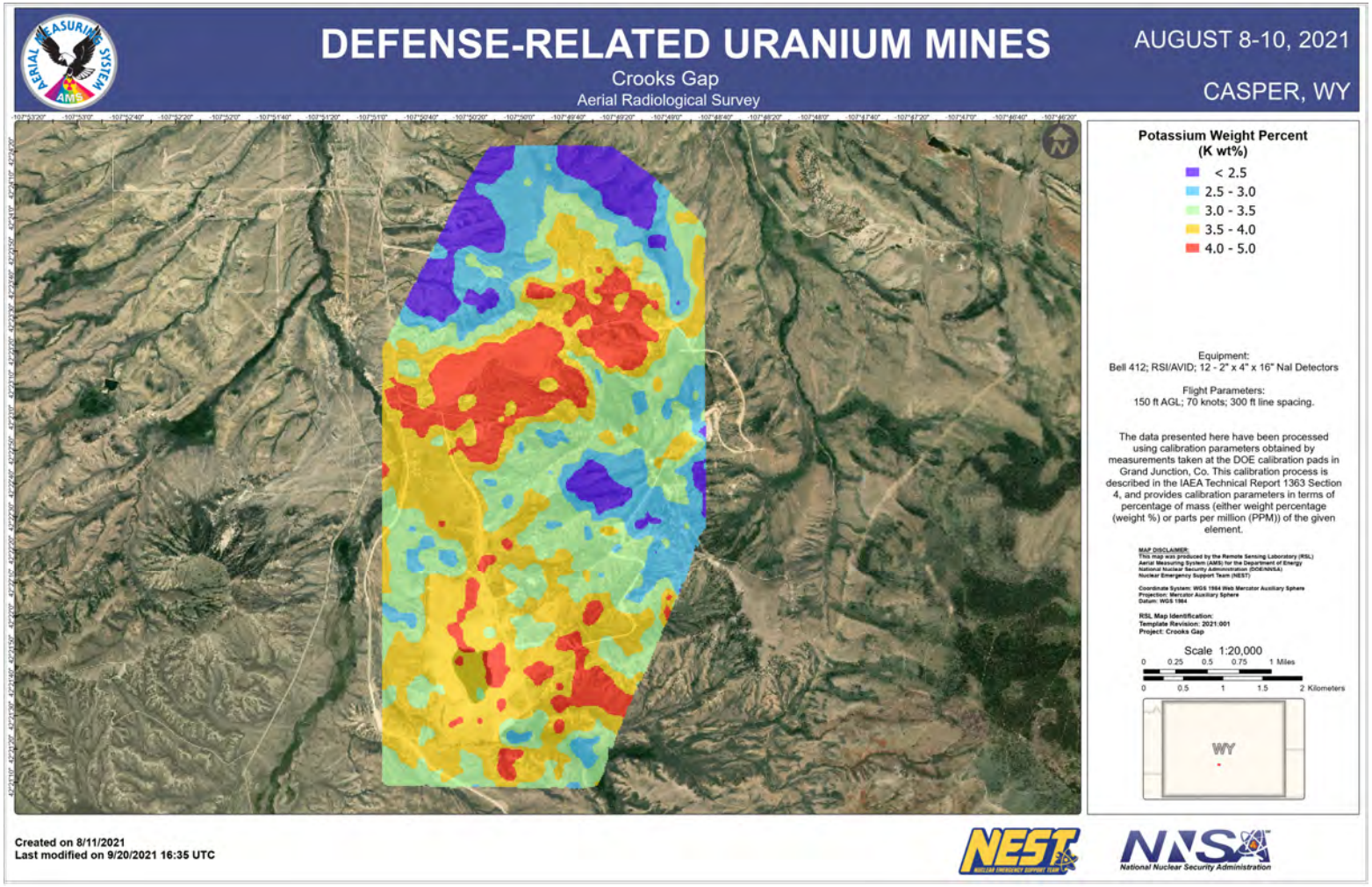

Figure 28: Potassium concentration results at Crooks Gap

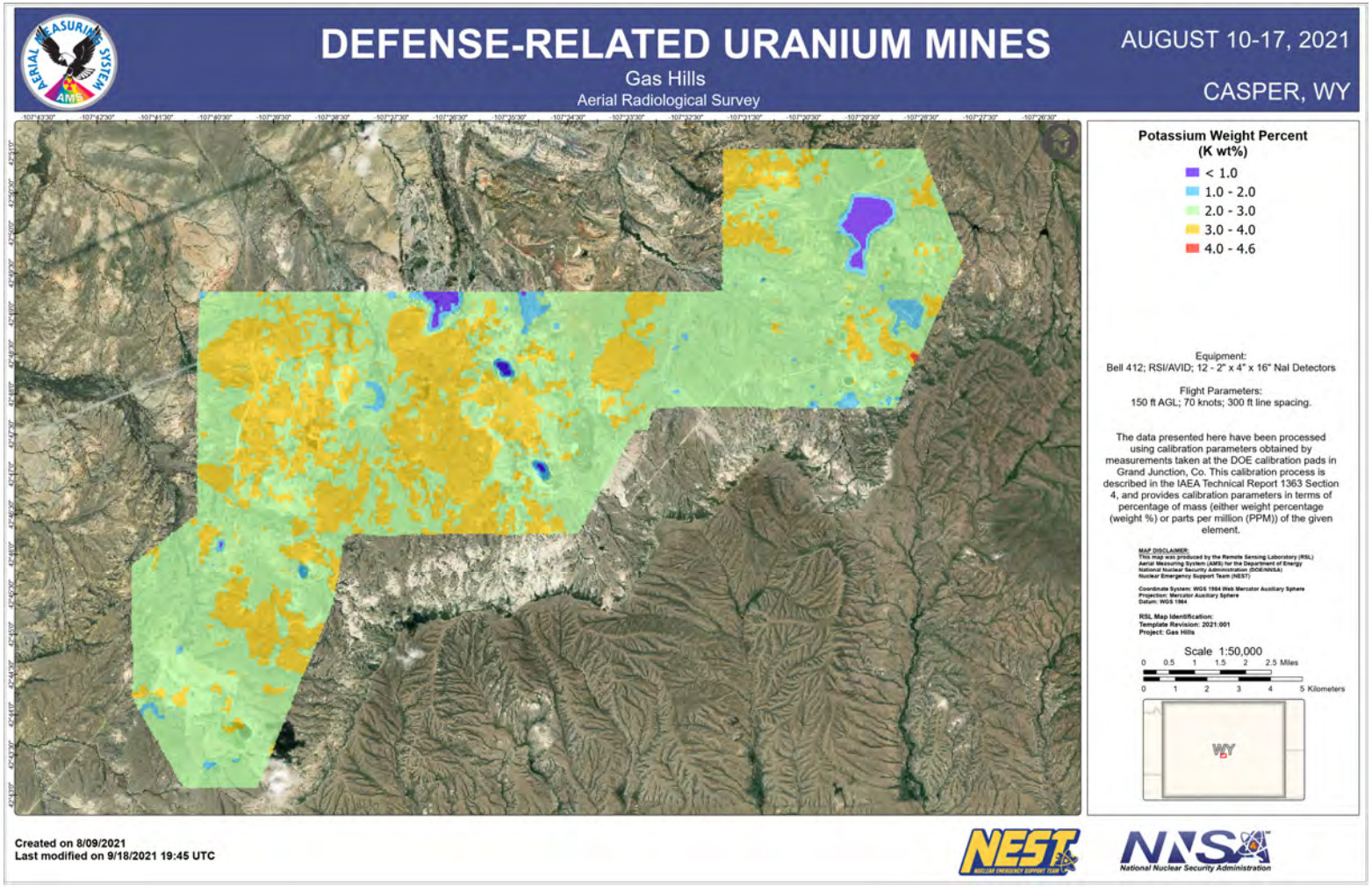

Figure 29: Potassium concentration results at Gas Hills

Mean spectral gamma data

Spectral gamma data were collected at a frequency of 1 Hz for every survey flight. Spectra were averaged in regions of similar exposure rate for the purpose of visualization. These mean spectra serve to highlight the differences in isotope mixture in various exposure rate regimes.

Shirley Basin

For the Shirley Basin survey the exposure rates varied from 3 to 55 μR/hr for areas not covered in water with no exposure rate data exceeding 64 μR/hr. A sample of averaged binned count rates from four representative regions in Shirley Basin is shown in Figure 30. The mean NaI(Tl) spectra show some variance in the spectral shape over these regions. High thorium levels on the east side led to natural exposure rates averaging 16 μR/hr and ranging up to 24 μR/hr despite nominal levels of U concentrations in that region that can be seen by comparing Figures and 21 and 24 . However, the highest exposure rates at Shirley Basin are clearly due to uranium concentrations (Figure 18). The mean gamma spectra for the 40 μR/hr average zone for both HPGe and NaI(Tl) measurements are shown in Figure 31 on the same count rate scale. The high resolution HPGe spectra were used to confirm the correct identification of gamma peak energy.

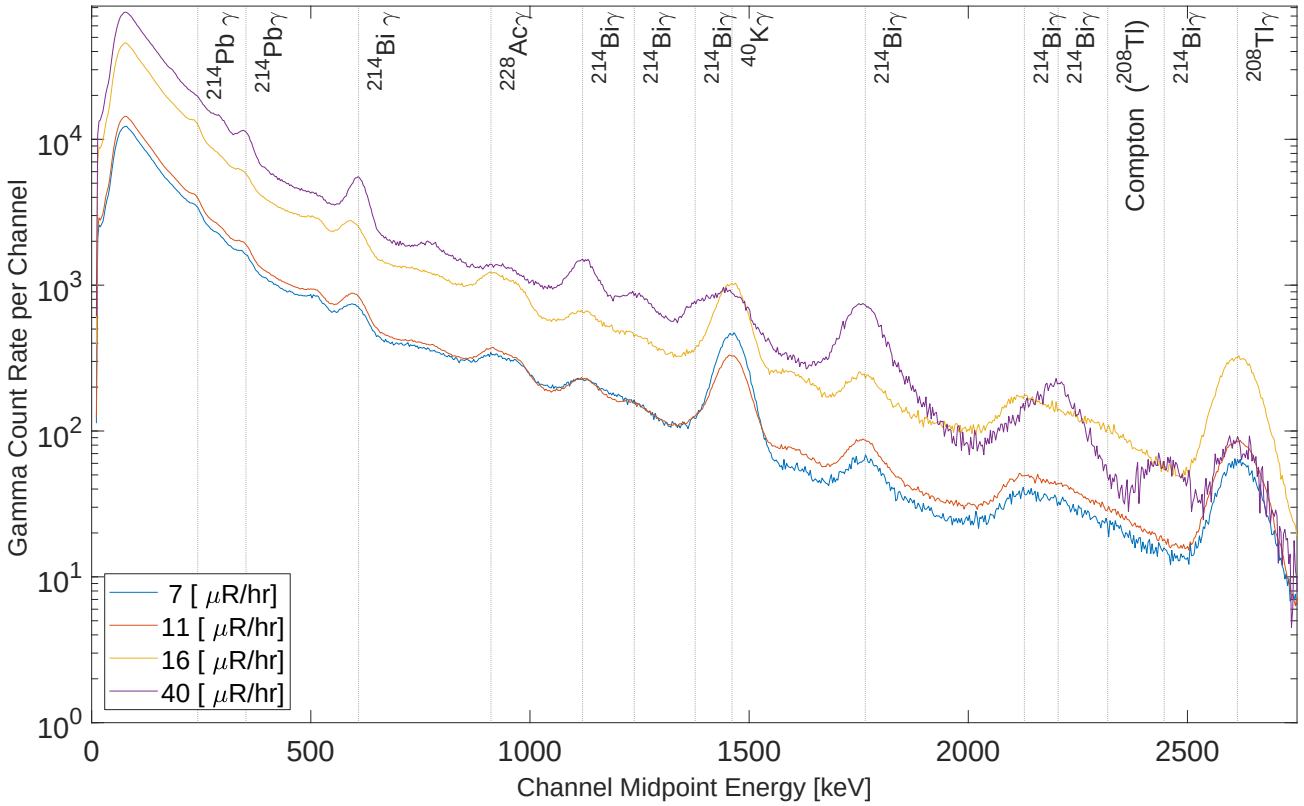

Figure 30: Comparison of mean NaI spectra gamma data at Shirley Basin

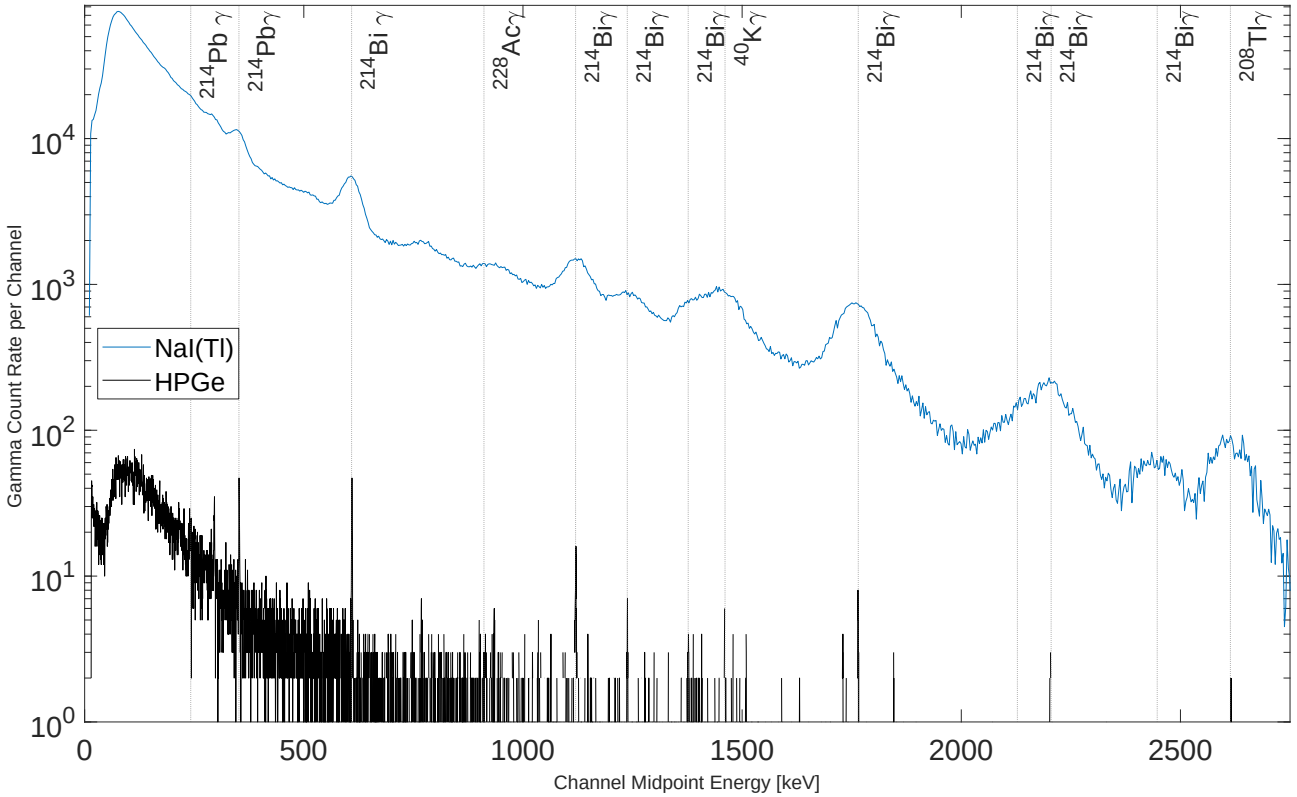

Figure 31: Comparison of mean NaI and HPGe spectra corresponding to a 40 μR/hr average exposure rate at Shirley Basin

Crooks Gap

The exposure rates for Crooks Gap ranged from 7 to 190 μR/hr. Three regions were sampled corresponding to areas with mean exposure rates ranging from 10 to 120 μR/hr. The mean NaI(Tl) spectra are shown in Figure 32, and a comparison of the HPGe and NaI(Tl) mean gamma spectra are shown for the 120 μR/hr averaged zone in Figure 33.

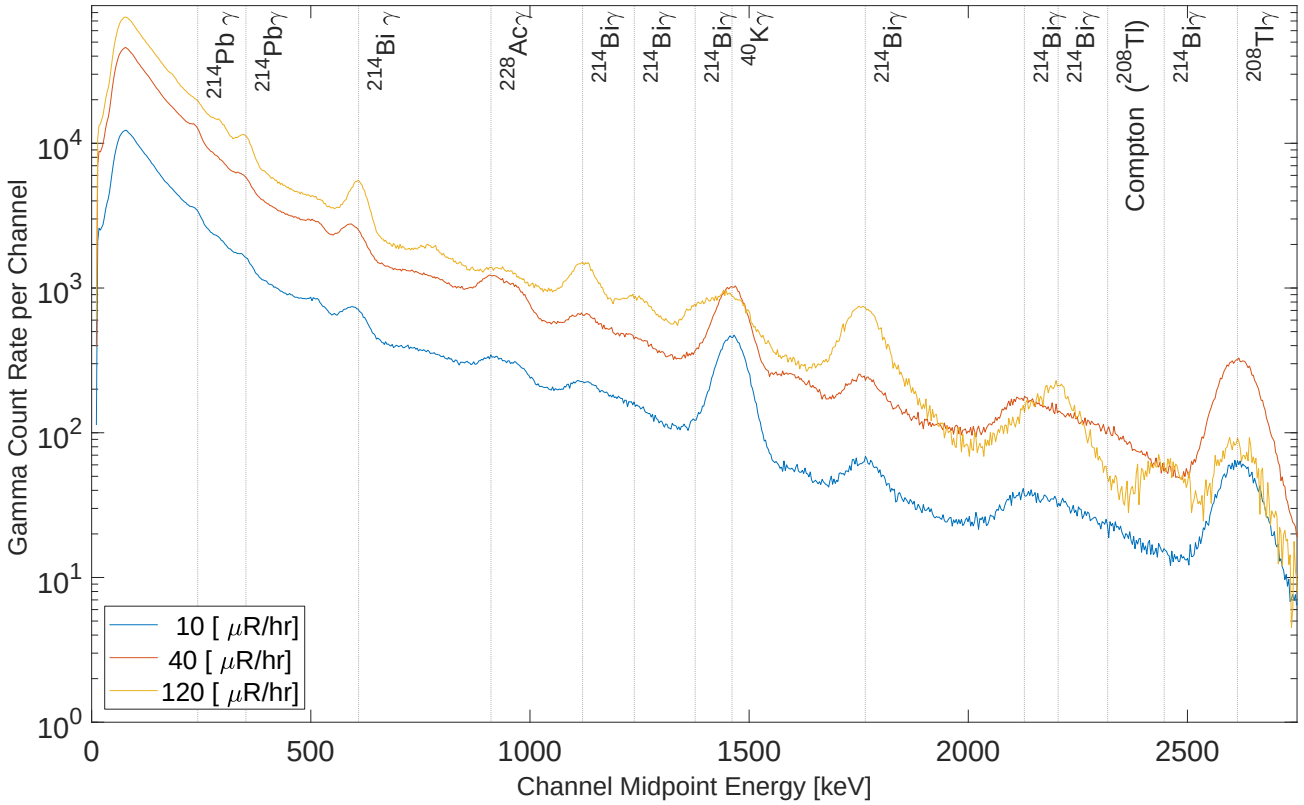

Figure 32: Comparison of mean NaI spectra gamma data at Crooks Gap

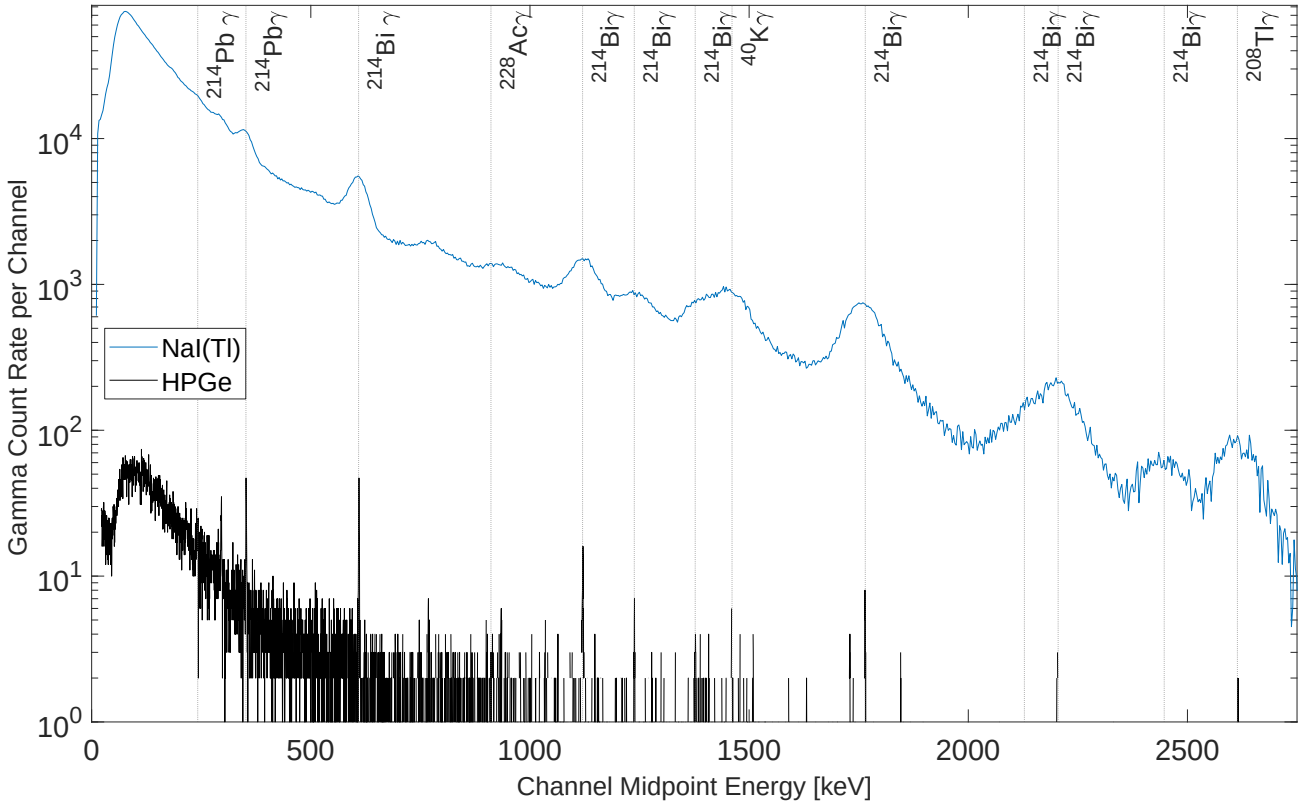

Figure 33: Comparison of mean NaI and HPGe spectra corresponding to a 40 μR/hr average exposure rate at Crooks Gap

Gas Hills

The exposure rates for Gas Hills ranged from 2 (in the remediated zones) to 140 μR/hr. Two regions were sampled corresponding to areas with mean exposure rates of 4 and 100 μR/hr. The mean NaI(Tl) spectra are shown in Figure 34.

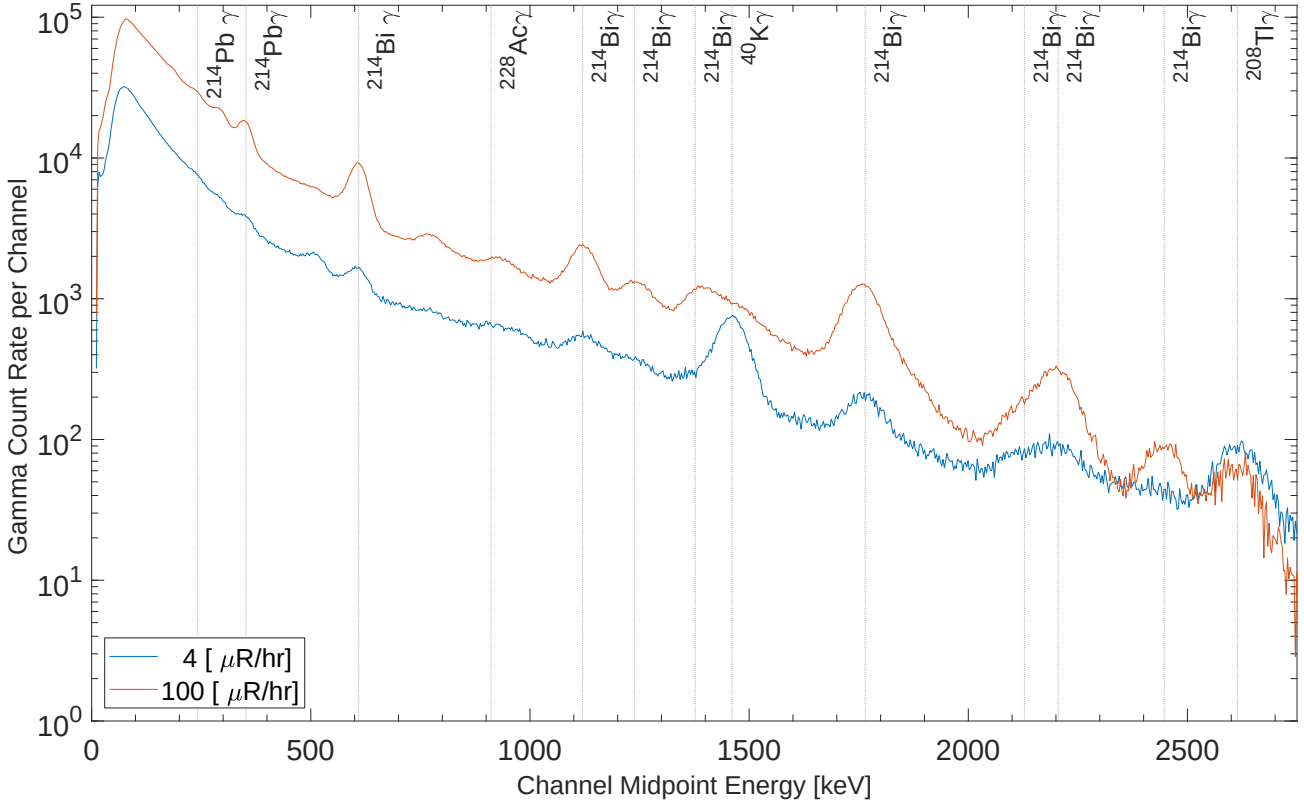

Figure 34: Comparison of mean NaI spectra gamma data at Gas Hills

Conclusion

The AMS survey team successfully completed sixty total hours of flight time in 12 days. Twenty-three hours of the flight time were directly over the survey areas of interest. The survey spanned 50,000 acres over the Shirley Basin, Crooks Gap, and Gas Hills DRUM sites, fully covering the Office of Legacy Management (LM) requested survey areas. The AMS survey results at Shirley Basin, Crooks Gap, and the Gas Hills are of sufficient quality to indicate that the exposure rates on the ground in these areas are within the acceptance criteria specified by LM. All survey measurements were below the 256 μR/hr upper threshold for total terrestrial exposure rate, indicating a reduced need for extensive further ground-based measurement. The survey data can be used to target ground sampling campaigns to areas of interest.

Appendix

Spectral extraction methods

AMS uses spectral extraction methods and empirical conversions approximations to determine terrestrial exposure and isotopic concentrations. The standard methods are the IAEA method and the Gaussian Method. These spectral based empirical correlations for the AMS detection system were determined from calibration at the Grand Junction LACP. The process requires cancellation of cosmic, aircraft, and radon background contributions which must be subtracted before any calibration can be performed. For calibration at the Grand Junction LACP, Pad 1 was treated as a background measurement pad. Ground measurements on Pad 1 were subtracted from each subsequent pad to generate a net concentration and net spectral measurement. This method of background subtraction is valid for both the IAEA and Gaussian methods. The resulting net extraction and concentrations were calculated as follows:

$$\Delta n_{ei} = n_{ei} - n_{e1} \tag{A.1}$$

and

$$\Delta c_{ei} = c_{ei} - c_{e1} \tag{A.2}$$

Where: n_{ei} = mean count extraction in an energy region for pad i
n_{e1} = mean count extraction in the background pad in an energy region
Δn_{ei} = background adjusted mean counts in an energy region for pad i

and

Where: c_{ei} = concentration of an element in pad i
c_{e1} = concentration of an element in the background pad
Δc_{ei} = background adjusted concentration of an element for pad i

IAEA method

The IAEA method requires the building of a matrix of sensitivities that allows for the estimation of scatter present in lower energy regions attributable to a specific higher energy regions per concentration. A mean spectra is calculated from the compiled dataset for each pad. For each mean spectra, the sum of the counts in each window is determined by:

$$n_e = \sum_{c=a}^{b} s_c \tag{A.3}$$

Where: s_c = the raw spectrum in channel c
n_e = the point-wise sum of counts in an energy region related to each isotope e where $e = (K, U, Th)$
a = the lower level discriminator
b = the upper level discriminator

The exact procedure to build the matrix is outlined in [4]. Briefly, the matrix of sensitivities is estimated by:

$$S \approx \Delta N \Delta C^{-1} \tag{A.4}$$

Where: S = the 3x3 matrix of sensitivity
ΔN = the 3x3 matrix of background adjusted mean count rate per characteristic region
ΔC = the 3x3 matrix of background adjusted concentrations

Equation (A.4) taken from [4]. Note that the 3x3 matrices given by N and C consist of columns composed of counts and concentrations respectively for K, U, and Th respectively; and rows that are from pads two, four, and three when considering the Grand Junction pads. The resulting matrix S is in terms of counts per concentration.

Gaussian method

Fitting a Gaussian to a peak of interest is used to determine the net counts in a photo-peak region of interest. The sum of the continuum and Gaussian response is fit to the experimental data. The Gaussian is then integrated to determine the net peak area in the region of interest.

Equation A.5 describes fitting the Gaussian with five degrees of freedom. After the initial fitting of a mean spectrum the two discriminator variables are held constant.

$$n(E) \approx a + bE + ce^{\frac{(E-E_0)^2}{2\sigma^2}} \tag{A.5}$$

Where: $n(E)$ = energy dependent raw spectral response
a = the lower level discriminator
b = the upper level discriminator
c = the Gaussian peak height
σ = the peak standard deviation
E_0 = the peak centroid

To determine the calibration parameters for K, eU, and eTh the result of the extraction performed by Equation A.5 is background subtracted according to Equation A.1. The sensitivity is then defined by the proportionality constant between a known concentration and counts in the energy region:

$$\alpha_e = \frac{\Delta c_e}{\Delta n_e}, \text{ where } e = (K, eU, eTh) \tag{A.6}$$

Where α has units of concentration per count of atomic weight percent potassium per net K window counts per second [K(Wt%)/ K cps], parts per million uranium equivalent per net U window counts per second [eU(ppm)/ U cps], and parts per million thorium equivalent per net Th window counts per second [eTh(ppm)/ Th cps].

Extraction parameters from the Grand Junction pad data and the calibration line

The calibration parameters determined by the IAEA and Gaussian methods were first tested against the Grand Junction LACP calibration pads. The same count extractions performed to determine the calibration parameters were used to calculate the concentrations of each pad on a point-wise basis (each spectra being an element). The results compared well to the publish pad data.

Windowed count data are altitude corrected for both the standard AMS exposure rate method and the isotopic concentration extractions calculated by the methods outlined in Sections A.2 and A.3. The counts in each region of interest were corrected for non-terrestrial

background by subtraction from data acquired over an adjacent body of water (the Pathfinder Reservoir) or a high altitude line. For water line data, the background data were acquired at the same survey altitude as the survey itself. After the counts in each region of interest were extracted and background corrected, the data was exponentially scaled to the ground according to the equation in Equation A.7.

$$f_{e,cal} = \alpha(f_e - f_{e,0})e^{\mu(z-z_0)} \tag{A.7}$$

Where:
- $f_{e,cal}$ = is the point-wise calibrated value for the appropriate element at ground level
- f_e = is the point-wise detector measurement value for the appropriate element at the aircraft height
- α = empirical conversion coefficient
- $f_{e,0}$ = is the point-wise calibrated background value for the appropriate element at the aircraft height
- μ = the energy dependent height attenuation coefficient in m^{-1}
- z = the height above ground in meters
- z_0 = reference altitude to which the calibrated conversion correction is applied (typically 1-m AGL)

After extracting and scaling the concentrations to the ground, aerial data points whose footprints overlap with the location of the ground truth samples were averaged to provide a single point of comparison and compared to the prediction from the aerial measurement.

Gridding and interpolation methods for contoured map data

AVID has built in interpolation method for rapid generation of rasters from processed aerial measurement data. A preferred gridding is based on a Gaussian Kernel weighting function ([14]). The application of this function results in 2-dimensional Gaussian smoothing optimized to air frame field of view. The smoothing process averages grid points with their spatial neighbors. This method does have the effect of blurring the sharp edges in the smoothed data. Smoothing is sometimes referred to as filtering, because it has the effect of suppressing high frequency signal like the stochasitic noise inherent in gamma radiation measurement, and enhancing low frequency signal . Other interpolation methods available in AVID and ArcGIS Pro include Inverse Distance Weighting and Kriging methods. The Gaussian interpolation is preferred by AMS as the smoothing process is analogous to the physical nature of the gamma signature measured by the detector system.

Attribution

Technical Staff	Role
Avery A. Bingham	Mission Manager/Chief Data Analyst
Daniel Haber	Data Analyst/GIS
Jez Stampahar	Data Analyst/GIS
Garrett Dean	Data Analyst/Ground Measurement
Chris Joines	Equipment Specialist
Edward Bravo	Equipment Specialist

Aviation Staff	Role
Michael Toland	Pilot in Command
Susan Roberts	Second-in-Command
Alex Brid	Alternate Pilot
Michael Hawkins	Mechanic

Acronyms

AEC	U.S. Atomic Energy Commission
AGL	above ground level
AMS	Aerial Measuring System
AVID	Advanced Visualization and Integration of Data
BLM	Bureau of Land Management
DGPS	Differential Global Positioning Systems
DOE	United States (U.S.) Department of Energy
DRUM	Defense-Related Uranium Mines
DSP	Digital Signal Processor
eTh	equivalent thorium
eU	equivalent uranium
FPGA	Field-Programmable Gate Array
FY	fiscal year
GIS	geographic information system
HPGe	high purity germanium
IAEA	International Atomic Energy Agency
ICP-MS	inductively coupled plasma mass spectrometry
K	potassium
LACP	Large Area Calibration Pads
LM	Office of Legacy Management
LMCL	Lake Mohave calibration line
LMTL	Lake Mohave test lines
MSL	mean sea level
NaI(Tl)	thallium doped sodium iodide
NASVD	Noise Adjusted Single Value Decomposition
NNSA	National Nuclear Security Administration
NORM	naturally occurring radiological material
PIC	pressurized ion chamber
PNNL	Pacific Northwest National Laboratory
ppm	parts per million
RSI	Radiation Solutions Incorporated
RSL	Remote Sensing Laboratory

TENORM	technologically-enhanced NORM
Th	thorium
U	uranium
U.S.	United States
Wt%	weight percent

References

[1] L. I. Boltneva, I. M. Nazarov, and SH. D. Fridman. "The cosmic radiation dose at the Earth's surface". In: *Izvestiya (English edition)* 4 (1974), pages 250–255.

[2] Hendricks T.J. Colton D.P. *Radiological Characterization of the Lake Mohave Test Line*. Technical report DOE/NV/11718-024. 1999.

[3] M Eisenbud. *Environmetal Radioactivity from Natural, Industrial, and Military Sources*. Volume Third Edition. London: Academic Press Inc., 1987.

[4] G Erdi-Krausz et al. *Guidelines for radioelement mapping using gamma ray spectrometry data*. International Atomic Energy Agency (IAEA), 2003.

[5] GE Oil & Gas. *RSS-131-ER / RSS-131 user's manual Rev. R*. General Electric Company. 8499 Darrow Road Twinsburg, OH 44087, 2014.

[6] Daniel A Haber, Mark A Norsworthy, and Avery A Bingham. "AMS / BARC Joint Survey Addendum Technical Report". In: (2021). URL: https://www.osti.gov/biblio/1785495.

[7] Daniel A. Haber, Russell L. Malchow, and Pamela C. Burnley. "Monte Carlo simulations of the gamma-ray exposure rates of common rocks". In: *Journal of Environmental Radioactivity* 167 (2017), pages 20–25. DOI: 10.1016/j.jenvrad.2016.11.013.

[8] Daniel A. Haber et al. "Modeling background radiation in Southern Nevada". In: *Journal of Environmental Radioactivity* 171 (2017), pages 41–64. DOI: 10.1016/j.jenvrad.2017.01.020.

[9] IAEA1363. *Guildelines for radioelement mapping using gamma ray spectrometry data*. Technical report IAEA-TECDOC-1363. 2003.

[10] Brian Minty and Jens Hovgaard. "Reducing noise in gamma-ray spectrometry using spectral component analysis". In: *Exploration Geophysics* 33.3-4 (2002), pages 172–176. DOI: 10.1071/eg02172.

[11] Brian Minty and Phil McFadden. "Improved NASVD smoothing of airborne gamma-ray spectra". In: *Exploration Geophysics* 29.3-4 (1998), pages 516–523. DOI: 10.1071/eg998516.

[12] I. Nirdosh. "Radium in uranium mill tailings-some observations on retention and removal". In: *Hydrometallurgy* 12 (1984), pages 151–176.

[13] RSI. *Airborne Radiation Solutions @ONLINE*. 2011. URL: https://www.radiationsolutions.ca/airborne/.

[14] Schabenberger. *Statistical methods for spatial data analysis*. Boca Raton: Champan & Hall, 2005.